

Reducing the squeak and rattle risk by improving the dynamic response and geometric variation in an assembly using topometry optimisation

Karl Lindkvist and Minh Tang

DIVISION OF PRODUCT DEVELOPMENT | DEPARTMENT OF DESIGN SCIENCES
FACULTY OF ENGINEERING LTH | LUND UNIVERSITY
2021

MASTER THESIS



Reducing the squeak and rattle risk by improving the dynamic response and geometric variation in an assembly using topometry optimisation

Karl Lindkvist and Minh Tang



LUND
UNIVERSITY

Reducing the squeak and rattle risk by improving the dynamic response and geometric variation in an assembly using topometry optimisation

Copyright © 2021 Karl Lindkvist and Minh Tang

Published by

Department of Design Sciences
Faculty of Engineering LTH, Lund University
P.O. Box 118, SE-221 00 Lund, Sweden

Publicerad av

Institutionen för designvetenskaper
Lunds Tekniska Högskola, Lunds universitet
Box 118, 221 00 Lund

Subject: Product Development (MMKM05), Technical Design (MMKM10)

Division: Product Development

Supervisor at LTH: Joze Tavcar

Supervisor at VCC: Mohsen Bayani Khaknejad

Examiner: Axel Nordin

Abstract

Squeak & Rattle are two types of undesired noise that occur in cars when components come in contact with each other, either impacting or sliding. It reduces the sense of quality and comfort for users, which are important aspects for premium cars. Two of the major contributors for generating squeak and rattle are geometric variation and insufficient stiffness, causing induced vibrations. This thesis aims to increase that stiffness by adding thickness to the inner door panel of a car. This is done by using a multi-disciplinary topometry optimisation approach which takes the geometric variation and the dynamic response into account.

The optimisation begins with an initial sensitivity analysis in order to apply the thickness to the most influential areas of the model. Topometry optimisation is then performed in multiple stages with constraints set to create a pattern of optimal thickened areas. Each stage of the optimisation uses a multi-objective genetic algorithm with an initial design of experiments population. Due to the time it takes to optimise a detailed model of the inner door panel, the development of the methodology is done by applying the optimisation on a simplified model.

The adding of thickness to a component changes the modal behaviour, resulting in a very sensitive optimisation process. However, the approach proved to be successful for both the simplified and complete model with a reduction of both of the optimisation objectives. The resulting thickness differed between the models, although for both models it had better effect on the objectives to increase the global stiffness rather than increasing the stiffness locally, near the fasteners.

Keywords: Squeak & Rattle, Modal analysis, Geometric variation, Multidisciplinary optimisation, Topometry optimisation, Multiple optimisation stages

Sammanfattning

Gnissel & skrammel är två typer av oönskat buller som uppstår i bilar när komponenter kommer i kontakt med varandra, antingen genom stötar eller glidning. Det minskar känslan av kvalitet och komfort för användare, som är viktiga aspekter för premiumbilar. Två av de viktigaste anledningarna till uppkomsten av gnissel och skrammel är geometrisk variation och otillräcklig styvhet, vilket orsakar inducerade vibrationer. Detta examensarbete syftar till att öka styvheten genom att addera tjocklek på bilens innerdörrpanel. Detta görs med hjälp av en multidisciplinär optimeringsmetod för topometri som tar hänsyn till de satta målen för den geometriska variationen och den dynamiska responsen.

Optimeringen börjar med en initial känslighetsanalys för att applicera tjockleken på de mest inflytelserika områdena i modellen. Topometrioptimering utförs sedan i flera steg med begränsningar satta för att skapa ett mönster av optimala förtjockade områden. Varje steg i optimeringen använder en multidisciplinär genetisk algoritm med en initial försökplanerings-population. På grund av den tid det tar att optimera en detaljerad modell av innerdörrpanelen, utvecklas metodiken genom att använda optimeringen på en förenklad modell.

Att addera tjocklek på en komponent ändrar det modala beteendet, vilket resulterar i en mycket känslig optimeringsprocess. Dock visade sig metoden vara fungerande för både den förenklade och fullständiga modellen med en minskning av båda målen. Den resulterande tjockleken skilde sig mellan modellerna, även om det för båda modellerna hade bättre effekt på målen att öka den globala styvheten snarare än att öka styvheten lokalt, nära fästpunkterna.

Nyckelord: Gnissel & skrammel, modalanalys, geometrisk variation, multidisciplinär optimering, topometrioptimering, flertal optimeringsfaser

Acknowledgements

We would like to express our deep gratitude to our supervisor from the Solidity department at Volvo Car Corporation (VCC), Mohsen Bayani Khaknejad, for his continuous support and creative ideas. He has also framed the conceptual idea for this work, making it possible for us to perform our master thesis at VCC.

We would also like to thank Lars Lindkvist, who has been giving us advice on encountered problems and difficulties with the RD&T software as well as helping us with implementing and updating new versions of RD&T according to our requirements. Furthermore, we would like to thank our supervisor at Lund University, Joze Tavcar, for his kindness and willingness to take his time to help us.

Last but not least, we would like to thank our friends and family for their support and advice throughout the thesis work.

Lund, February 2021

Karl Lindkvist, Minh Tang

Contents

1	Introduction	10
1.1	Background	10
1.2	Objective and research questions	10
1.3	Assumptions	11
1.4	Limitations	11
1.5	Structure of the thesis	12
2	Theory	13
2.1	Squeak and Rattle	13
2.2	Modal analysis	14
2.2.1	Eigenfrequencies and Eigenmodes	14
2.2.2	Dynamic stiffness	15
2.2.3	Resonance	16
2.2.4	Resonance risk	17
2.2.5	Modal Assurance Criterion	19
2.3	Geometric variation	19
2.3.1	Tolerances	20
2.3.2	Robust design	20
2.3.3	Robust Design & Tolerancing	20
2.4	3-2-1 Locating Principle	21
2.5	Design of Experiments	23
2.5.1	Latin Hypercube	23
2.5.2	Incremental Space Filler	24
2.5.3	Plackett-Burman	24
2.5.4	Foldover Design	25
2.6	Multidisciplinary optimisation	25
2.6.1	Multi-Objective Genetic Algorithm	26
2.6.2	modeFRONTIER	28
2.7	Topometry Optimisation	28
2.7.1	Previous studies on topometry optimisation	29
2.7.2	Adding rigidity	30
3	Methodology	31
3.1	Optimisation problem	31

3.1.1	Geometric variation	32
3.1.2	Dynamic response	32
3.1.3	Multi-Disciplinary Optimisation	32
3.1.4	Weighting of objectives	32
3.2	Sensitivity analysis	33
3.2.1	Evaluating Analysis Methods	33
3.2.2	Identifying relevant design variables	36
3.3	First Optimisation Stage	40
3.3.1	Property identification number	41
3.3.2	Modified Incremental Space Filler	42
3.3.3	Initial design of experiments size	42
3.3.4	Number of generations	43
3.3.5	Selection of the best candidate on the Pareto front	44
3.4	Further Optimisation Stages	44
3.5	Constraints	44
3.5.1	Sorting	45
3.5.2	Proximity	45
3.5.3	Mass	46
3.6	Flow charts	47
4	Modelling	49
4.1	Model selection	49
4.2	CBUSH	50
4.3	PSHELL	50
4.4	Modified fasteners	51
4.5	Configuration 3	53
4.5.1	Fasteners	54
4.5.2	Refinement after Sensitivity analysis	55
4.5.3	Refinement after first optimisation stage	57
4.5.4	Refinement after second optimisation stage	59
4.5.5	Refinement after third optimisation stage	61
4.6	Side door	63
4.6.1	Fasteners	66
4.6.2	Refinement after the sensitivity analysis	67
4.6.3	Refinement after first optimisation stage	68
5	Results	71
5.1	Configuration 3	71

5.2	Side door	75
6	Discussion	81
6.1	Configuration 3	81
6.2	Side door	82
7	Conclusions	84
8	Sources of error	85
9	Future recommendations	86
	References	87
	Appendix A Work distribution and time plan	92

List of acronyms and abbreviations

ABS	Acrylonitrile butadiene styrene
CA	cellular automaton
CAT	computer aided tolerance
DOE	design of experiments
FEA	finite element analysis
HCA	hybrid cellular automaton
ISF	incremental space filler
MAC	modal assurance criterion
MDO	multidisciplinary optimisation
MOGA	multi-objective genetic algorithm
PID	property identification number
RD&T	robust design & tolerancing
S&R	squeak and rattle
ULH	uniform latin hypercube
VCC	Volvo Car Corporation

1 Introduction

The introduction aims to give the reader an overview of squeak and rattle, research questions, possible assumptions and limitations.

1.1 Background

Squeak & Rattle (S&R) are non stationary sounds that occur when adjacent parts come into contact, either impacting or sliding. A car with in-cabin S&R problems is considered quality deficient and with the current emphasis on electrification, the non stationary noises in the car cabin will further draw the attention of passengers.

One of the main sources for the generation of S&R in the car cabin is geometric variations. This can result from manufacturing tolerances or other variation sources like temperature or ageing [15]. Previous methods that have been used to minimise the geometric variations include optimisation of attachment points, adjusting the tolerance levels for a robust design and optimising the assembly procedure. However, optimising the attachment points affects the dynamic response. It is therefore necessary to take this effect into account in the optimisation. In this thesis work, topometry optimisation is used to minimise the risk for squeak and rattle. This approach designs the thickness of each element individually. Furthermore, the optimal attachment points found in the previous project at Volvo Car Corporation, VCC, are included in the optimisation.

1.2 Objective and research questions

The main objective of this thesis is to develop an optimisation workflow for multi-objective topometry optimisation of an assembly developed for geometric variation and dynamic response analyses.

A further minor research question is also analysed:

- How does the results from the multidisciplinary topometry optimisation vary between the simplified geometries and their corresponding realistic models?

1.3 Assumptions

The models, mesh and original workflows in the software modeFRONTIER, provided by VCC and previous thesis students at VCC, are assumed to be correctly built and accurate.

1.4 Limitations

Several software used at VCC are limited. The latest available version of MATLAB on the server is 2015b, making some commands in later versions not available. This version of MATLAB is used internally in the software modeFRONTIER. The software used for geometric variation, RD&T, is also limited by the current functions. However, some limitations in RD&T have been solved by implementing new functions and updating the software.

Due to computational limitations and limited RAM on the provided VCC laptops, the computational time in RD&T was high since it was time consuming to calculate the stiffness matrix for the more complex models.

Time constraint is also a major limitation in this thesis work. Due to limited time, only two models were studied, one simplified model (configuration 3) and one complete model (the side door). Further models are available at VCC and have been studied in previous projects. Time is also a factor for several choices in this thesis work, such as the number of designs, generations and optimisation stages, which are described later on in this report.

1.5 Structure of the thesis

This report begins with an introduction and then presents some relevant theory and the research that has been done for this thesis work. The research covers the parameters that have an impact on squeak and rattle, but also previous studies on topometry optimisation in various contexts.

After the theory, the methodology is presented. Initially the problem is formulated, followed by an explanation of the steps for solving it. Modelling is the next chapter and it describes the models used in this thesis work. It starts with a presentation of some important properties of the models and then continues to describe how the models were edited between the optimisation stages.

The results are thereafter presented, first for the simplified model and then for the full model. The results are followed by a discussion part, where each model have their own section. The discussion is followed by some conclusions and the sources of errors as well as recommendations for future work. The final parts are references and appendices.

2 Theory

This chapter contains relevant literature study and research of squeak and rattle, modal analysis, geometric variation, fasteners, design of experiments and optimisation algorithms as well as previous work on topometry optimisation.

2.1 Squeak and Rattle

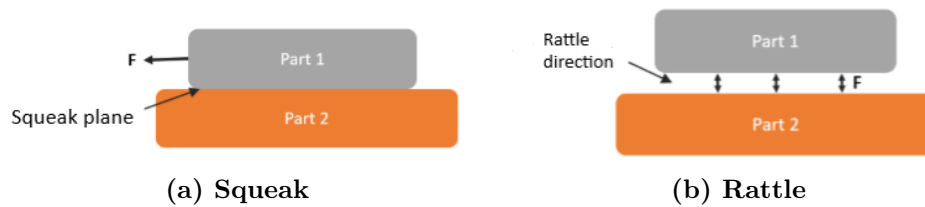


Figure 1: Squeak and Rattle [16]

Squeak, seen in Fig. 1a, is an undesired noise caused by induced friction of two different parts sliding relatively against each other. The contact surfaces stores energy during elastic deformation which is released when the static friction exceeds the kinetic friction [15]. The released energy produces the squeak noises. The amplitude and frequency of squeak are generated by many factors such as material properties, coefficient of friction, sliding velocity, normal load and wear characteristics.

Rattle, seen in Fig. 1b, is another undesired noise that occurs when there is an impact between two hard surfaces and the motion is relative. Rattle is generally caused by loose or overly flexible elements under forced excitation. The impacts occur due to inertial vibration between two components if the tolerances are poor, vibration is excessive or subassemblies are very close. Rattle is primarily induced by road excitation of the vehicle.

S&R partly depends on geometric variations but may also occur when the relative motion exceeds a threshold value. The relative motions depend on insufficient stiffness, excessive input forces or poor modal alignment [15]. Low stiffness in a part contributes to large vibrations which when in contact with surrounding parts causes high squeak and rattle in the assembly [25].

2.2 Modal analysis

Modal analysis is used to formulate a mathematical model for a system's dynamic behaviour by determining the dynamic characteristics in terms of eigenfrequencies, damping factors and mode shapes [13].

The dynamic characteristics are used to describe a system's natural modes of vibrations, which are determined by the mass, stiffness, damping and spatial distributions. The natural modes of vibration can be expressed as the linear combination of a set of simple harmonic motions. The basis for modal analysis is the fact that these natural modes of vibration can be expressed by the vibration response of a linear time-invariant dynamic system.

2.2.1 Eigenfrequencies and Eigenmodes

The eigenfrequency is the frequency at which the structure tends to vibrate when subjected to external forces. For a single degree of freedom system, the eigenfrequency ω is defined as

$$\omega = \sqrt{\frac{k}{m}} \quad (1)$$

where k is the stiffness and m is the mass, depicted in Fig. 2.

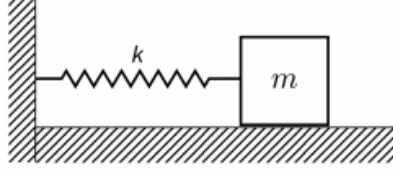


Figure 2: Spring-mass system [7]

The vibrational movement at a certain eigenfrequency is called eigenmodes. A structure usually has more than one eigenfrequency and thus multiple eigenmodes. Eigenmodes can give useful information of where modification is needed to reduce the vibration response [34].

2.2.2 Dynamic stiffness

Road excitation induces dynamic forces acting on a vehicle body and these forces depend on the interaction between road, tyres, chassis' components and vehicle body [28]. The dynamic stiffness k is described as the resistance to deformation from an input force and defined as

$$k = \frac{f}{x} \quad (2)$$

where f is the dynamic force and x is the displacement. The vibration of the structure can also be seen as the ratio of the forces acting on a structure to its stiffness, as seen in Fig. 3 [8]. Resonance occur at the valley in Fig. 3.

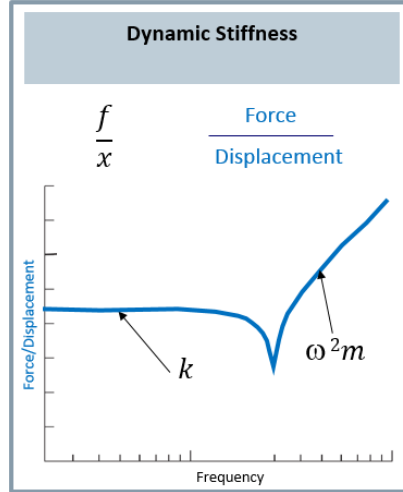


Figure 3: Dynamic stiffness [8]

2.2.3 Resonance

Resonance is a phenomenon that occurs when the forcing frequency is equal to or almost equal to the eigenfrequencies of the system. This results in large vibrations of the system. To avoid resonance, it is possible to alter the mass or stiffness, according to Eq. 1, to place the eigenfrequency above or below the forcing frequency [34].

Increasing the stiffness results in a higher eigenfrequency, see Eq. 1. The stiffness is inversely related to the displacement according to Eq. 2. Increasing the stiffness therefore implies to reduce the displacement. Using Eqs. 3, 4 and 5, one can see that decreasing the displacement u results in lower strain ε and stress σ , as Young's modulus E is constant, which in turn indicates larger cross-sectional area A (assuming constant periodic applied force N), thereby increased thickness [26]. Thus can topometry optimisation be used for the dynamic response analysis. According to Eq. 1, increasing the mass results in lower eigenfrequency, which usually is not a preferable method. One therefore has to find a balance between adding thickness to increase the eigenfrequency while taking the increase in mass into account.

$$\varepsilon = \frac{du}{dx} \tag{3}$$

$$\sigma = E\varepsilon \tag{4}$$

$$N = A\sigma \tag{5}$$

2.2.4 Resonance risk

The resonance risk is defined as the total number of resonant frequencies for all nodes in both normal (rattle) and planar (squeak) direction. In Fig. 4, the displacement is plotted against the frequency for the two parts of a model. The parts can be distinguished by the different colours black and green.

The mean line is the average value of the displacement for all measure points in the frequency span, seen in Fig. 4 as the black and green horizontal solid lines for respective part in the model. The percentile line, shown as the black and green horizontal dashed lines in Fig. 4, is determined by the percentile of each curve for all measure points [16]. The percentile can vary between the 10th to the 90th percentile.

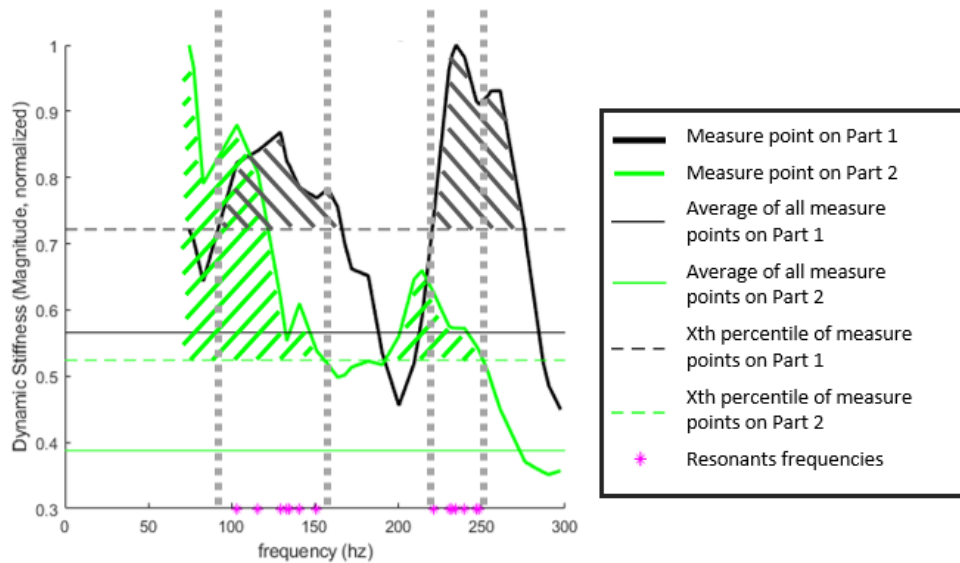


Figure 4: Dynamic stiffness plotted against frequency for resonance frequency identification [16]

Fig. 4 shows which eigenfrequencies that contributes to resonance. The black and green hatched portions show in which areas the eigenfrequencies are considered to be resonance contributors. This is determined by the dynamic stiffness value in relation to the percentile line and the mean line. The dynamic stiffness value needs to be above both of these lines to fulfill the criteria for creating resonance.

The resonance frequencies are shown as purple asterisks in Fig. 4 and the total number of resonances is the sum of these identified frequencies. By combining this number with displacement data and velocity data for each measure point, the resonance risk number can be calculated.

The resonance risk is calculated in MATLAB. The values of the mean line factor and percentile is based on the previous project at VCC. An analysis was performed in the previous project for all the different model configurations and the common sensitive area was identified when the mean line factor had a value of 0.7 with a 70th percentile, i.e. only the top 30% of the eigenfrequencies can contribute to resonance. These values were therefore chosen for all model configurations.

2.2.5 Modal Assurance Criterion

The modal assurance criterion, MAC, relates the degree of linearity between two modal vectors with one of them being the reference. MAC is defined according to Eq. 6 where Ψ is the eigenvector, such that it is normalized by the magnitude of the vector and thus, takes a value between 0 and 1 [1]. A MAC value close to zero indicates that the modal vectors are non-consistent, i.e. the mode shape vectors are linearly unrelated. If the different modal vectors are estimated at different excitation positions, then a MAC value close to zero implies orthogonal modal vectors. A MAC value close to unity however, indicates that the modal vectors are consistent, i.e. the correlation between them is linear.

$$MAC_{cdr} = \frac{|(\Psi_{cr})^T(\Psi_{dr}^*)|^2}{(\Psi_{cr})^T(\Psi_{cr})^*(\Psi_{dr})^T(\Psi_{dr})^*} \quad (6)$$

The MAC value should be maximised in terms of minimizing the S&R risk since in phase movement of the points on the interface is desired. The S&R risk is increased for out phase movements, i.e. low MAC value, since vibrations may occur. In order to be able to set the optimisation to minimise the value for S&R risk, the mode shape similarity number is used which is defined as the average value when taking 1 minus the weighted MAC vector.

2.3 Geometric variation

Geometric variation is among the major causes for the generation of squeak and rattle sounds in the car cabin and can be the result from manufacturing tolerances or other sources such as temperature or ageing. In an assembly consisting of several parts, the tolerances for each part create a tolerance stack-up. These stack-ups can magnify the dimensional variations in critical interfaces that generates squeak and rattle [3].

Using geometric variation simulations can help determine how the geometric variation is affected by different parameters. Increasing the stiffness in the optimal locations of a part can reduce the effect that the tolerances have on an assembly. In simplified terms, increased stiffness in the right locations can increase how well

parts fit together when being assembled, which in its turn reduces the risk for S&R.

2.3.1 Tolerances

Tolerances are one of the major factors influencing the geometric variation [17]. It is defined as the allowed geometrical variations from the nominal value of a feature in terms of the size, orientation and location.

A Six Sigma approach for the tolerance design can be a useful tool to reduce the geometric variation [38]. Geometric variation can also be reduced by reducing the deviation.

2.3.2 Robust design

A product that has a robust design is one that works as intended regardless of the geometric variations of the product. A robust design can be achieved by knowing the sources of variation and minimising the products sensitivity to these sources [23].

Using the approach to create a robust design can be a more cost efficient alternative to minimise the sensitivity to geometric variations from manufacturing tolerances, instead of lowering the tolerance itself.

2.3.3 Robust Design & Tolerancing

Robust design & tolerancing, RD&T, is a computer aided tolerance (CAT) software tool that is used to simulate statistical variation to visualise the effect of geometric variation from manufacturing and assembly long before physical prototypes are manufactured [32]. This enables the possibility to analyse and compare different design concepts improving the decisions made especially during early stages of product development.

RD&T uses Monte Carlo simulation to analyse variation statistically, the integrated finite element analysis (FEA) solver allows non-rigid analysis for assemblies

with sheet metal or plastic parts [31].

In RD&T, the geometric variation is analysed with a so called measure [17]. A measure is a critical point or dimension where variation of geometry is to be analysed, see Fig. 5. This measure is predefined and can be defined in several ways in RD&T, however Point-to-point measure is used in this thesis work. The Point-to-Point measure is defined as the distance between two nodes.

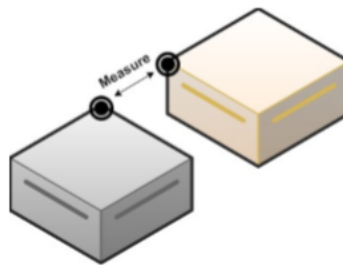


Figure 5: Illustration of a measure used in RD&T [17]

2.4 3-2-1 Locating Principle

When mounting a part in a fixture and restricting all six degrees of freedom so that the part cannot move, the 3-2-1 principle can be used. It uses six individual locators in three steps to reference and restrict the work piece [12]. The first step is to set three points on one surface to restrict three degrees of freedom. This is usually done on the largest surface of the part.

The second step is to set two points on a surface perpendicular to the first one. This restricts two further degrees of freedom with only one to go. The last one is restricted by adding one more point to a surface that is perpendicular to the other two. With that done the part is now fully constrained and unable to move along or rotate about the X, Y and Z axes. The 3-2-1 principle can be seen in Fig. 6.

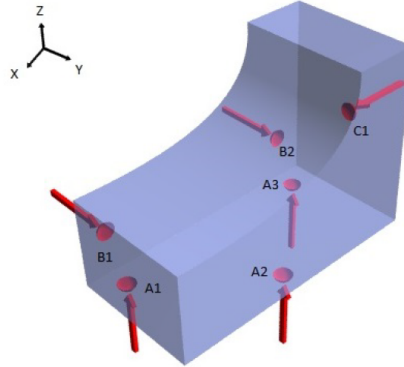


Figure 6: The 3-2-1 locating principle [21]

The 3-2-1 locating principle is not always suitable to use for thin shell and compliant objects due to their flexibility and low rigidity [12]. In these cases, the N-2-1 locating scheme can be used to compensate for the flexibility and the low rigidity. In this method, N supports instead of three are added to support the part in the primary datum direction to avoid excessive deflection. Fig. 7 shows an example of a N-2-1 locating scheme.

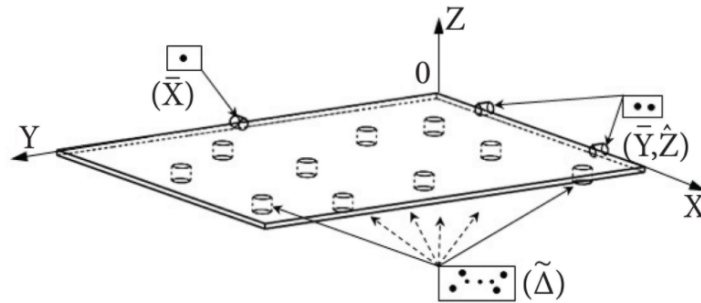


Figure 7: The N-2-1 locating principle [12]

2.5 Design of Experiments

Design of experiments (DOE) is a systematic method to determine how input factors affect a certain output [36]. In order to get an overview of the relationship between input and output without testing every possible combination, DOE combines the input variables in different ways and documents how it affects the output. With enough iterations, the behaviour of a system can be predicted. How the input variables are selected in the design space during these iterations can be done in several ways, two of which are described below.

2.5.1 Latin Hypercube

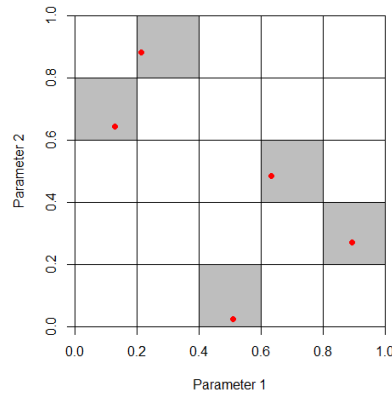


Figure 8: Uniform Latin Hypercube sample [5]

The design space is divided into orthogonal grids when using Latin Hypercube. The number of orthogonal grids depends on the number of input parameters. Only one sample is then chosen along each row and column and will be given a random value within this row and column, see Fig. 8. Uniform Latin Hypercube, ULH, ensures that samples are spread uniformly all over the design space. Latin Hypercube sampling is often used in Monte Carlo simulations and has variance reducing properties [33].

2.5.2 Incremental Space Filler

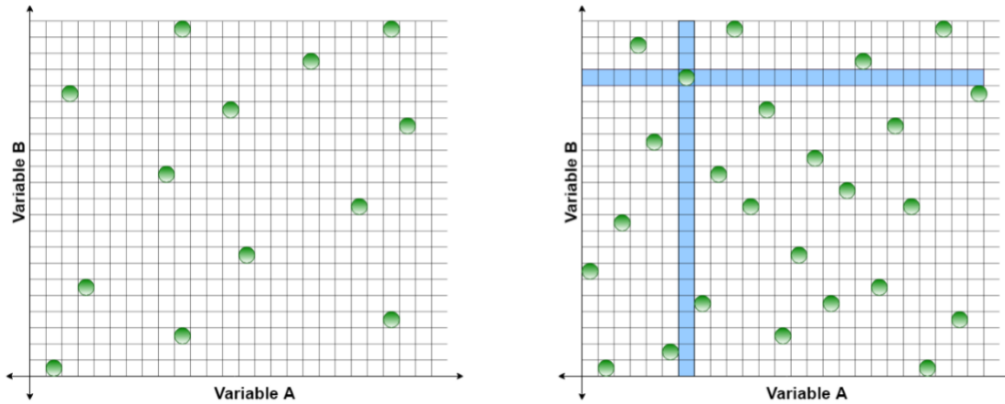


Figure 9: Incremental Space Filler

Incremental Space Filler (ISF) is an augmenting algorithm that aims to create a population in the design space as evenly spread out as possible. This is achieved by sequentially adding each new design samples with a maximised minimum distance from the previously added points in the design space, illustrated in Fig. 9. ISF is suitable for genetic algorithm optimisations [10].

2.5.3 Plackett-Burman

A Plackett-Burman design, mainly used for screening experiments, is a two-level fractional factorial design with $k = N - 1$ variables where N is the number of runs [22]. N can either be a power of 2 or a multiple of 4. The Plackett-Burman design is equivalent to other fractional factorial designs for $N = 2$, but is especially of interests if $N = 12, 20, 24, 28, 36$ and a multiple of 4. These type of designs are called nongeometric and cannot be represented as cubes. For $N = 12, 20, 24, 28, 36$, the design is constructed such that the next column is generated from the previous one by moving the elements of the column down one position and placing the last element in the first position. When k designs have been generated, one additional row is added, consisting of minus signs, see Fig. 10. The design can also be constructed by generating row by row, where the next row is generated by moving the elements of the row to the right and placing the

last element in the first position.

Run	A	B	C	D	E	F	G	H	I	J	K
1	+	-	+	-	-	-	+	+	+	-	+
2	+	+	-	+	-	-	-	+	+	+	-
3	-	+	+	-	+	-	-	-	+	+	+
4	+	-	+	+	-	+	-	-	-	+	+
5	+	+	-	+	+	-	+	-	-	-	+
6	+	+	+	-	+	+	-	+	-	-	-
7	-	+	+	+	-	+	+	-	+	-	-
8	-	-	+	+	+	-	+	+	-	+	-
9	-	-	-	+	+	+	-	+	+	-	+
10	+	-	-	-	+	+	+	-	+	+	-
11	-	+	-	-	-	+	+	+	-	+	+
12	-	-	-	-	-	-	-	-	-	-	-

Figure 10: Plackett-Burman design for N=12 runs and k=11 variables [22]

A Plackett-Burman design is a nonregular design that does not account for the effect of interactions between the variables. Moreover, Plackett-Burman is a design of resolution III where main effects are estimated but confounded with two-factor interactions and some two-factor interactions may be confounded with each other.

2.5.4 Foldover Design

A foldover design is obtained by reversing the signs of all the columns for a fractional factorial design and then adding the result to the fractional factorial design. By doing this, one can increase the resolution of a resolution III design, such as a Plackett-Burman, to a design of resolution IV. This means that in addition to the main effects, the effects from two-factor interaction are able to be estimated. It also clears the confounding between the two-factor interactions and the main effect [22].

2.6 Multidisciplinary optimisation

Multidisciplinary optimisation, MDO, involves optimisation of several objectives that usually conflict with each other. Due to this conflict, a candidate that excels

from one aspect lacks in another. This means that there is not a single best solution to a multi-objective optimisation problem. The most optimal candidates are distributed along a so called Pareto front [29].

2.6.1 Multi-Objective Genetic Algorithm

Multi-objective genetic algorithm, MOGA, is a population based optimization method that is used to solve multi-objective optimisation problems. MOGA-II is an improved version of the regular MOGA.

There are some key terms that are important in describing the structure and functionality of a genetic algorithm. Firstly, a design is referred to as an individual or chromosome. It is defined and separated from other individuals by its genes, i.e. the variables which optimal value is to be obtained. Several individuals together form a population. In order to start a MOGA, an initial population needs to be generated. These individuals are randomly generated based on target functions and restrictions.

The initial population forms the so called, first generation. A generation can be defined as a population at any given time and all generations consists of equally sized populations [37]. The first generation will be the basis for the next one and so on. The new individuals in the next generation are called children and they are based on their parents.

The best individuals of a generation are directly transferred to the next one. This is called elitism and helps to preserve the individuals closest to the Pareto front. The other individuals in the next generation are reproduced based on four different operators - one-point crossover, directional crossover, mutation and selection [29]. One operator is chosen at every reproduction step and is applied to the current individual. Which operator is chosen depends on the predefined operator probabilities. The four different operators are explained below.

One-point crossover is when the genetic material is exchanged between two different parents to create two new children. One of these is then randomly selected to be the new individual. An example is shown in Fig. 11.

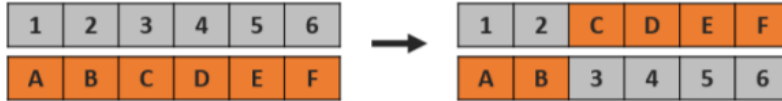


Figure 11: One-point crossover [16]

Directional crossover is similar to one-point crossover but it compares the fitness values of the two parents and tries to find a direction of improvement. The direction of improvement is randomly weighted and based on the direction vectors of the parents, see Fig. 12.

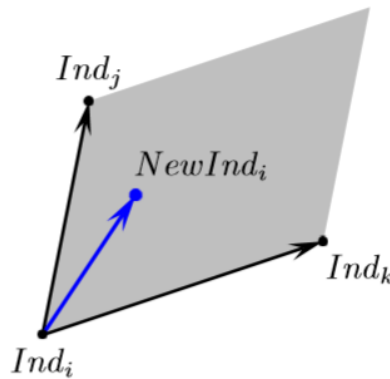


Figure 12: Directional crossover [29]

Selection is when a individual goes to the next generation without changing anything in its design.

Mutation diversifies one generation from the next. It changes one or several attributes to ensure that the new individual differs from the old one. DNA String Mutation Ratio is a value that gives the percentage of the attributes changed by the mutation [29]. Fig. 13 shows a graphical example of a mutation.



Figure 13: Mutation [16]

When a population of a whole generation is generated from these reproduction operators, the objective fitness function is calculated. All non-dominated designs are then added to the elite set which is repeatedly updated to preserve the fittest individuals. The new designs for the next generation are then created based on the individuals from the elite set and from individuals created by the operators. All these steps are repeated to create the specified number of generations.

2.6.2 modeFRONTIER

modeFRONTIER is developed by the independent software provider ESTECO. modeFRONTIER is a software used for multi-objective optimisations and MDO to cut time and cost. The optimal solutions are found on the Pareto front using a suite of DOE and optimisation algorithms. The simulation process is viewed in a so called workflow. modeFRONTIER combines multiple calculation tools and have effective tailor-made algorithms [27].

2.7 Topometry Optimisation

Topometry optimisation is an optimisation method where the dimensions, such as thickness of each element, are designed individually. Topometry optimisation is used if the structural shape, distances and the number of stiffeners must be kept [14]. It is often compared with topology optimisation which is better for creating rib patterns, while topometry optimisation is more suited for determining the optimum thickness within different regions of a part.

Optimising a design, element by element, can create a very time consuming optimisation process when working on larger models. Thus can clustering of the elements reduce computational time in the optimisation.

2.7.1 Previous studies on topometry optimisation

Topometry optimisation is less used than other optimisation methods, such as topology optimisation. Chandan K. Mozumder has used a modified Hybrid Cellular Automaton (HCA) algorithm for topometry optimisation for crashworthiness design where shell structures are involved [24]. The HCA algorithm is inspired by the biological phenomena of bone remodeling and based on the cellular automaton (CA) model. The CA model discretizes the design domain into a regular grid of cells. Each cell has a neighborhood and the state of the cell is updated based on the values in the neighborhood at previous time step. The final mass of the structure has also been taken into account. Common CA neighborhood layouts can be seen in Fig. 14 where the number of elements in the neighborhood are denoted as \hat{N} . The von Neumann has been used in the dissertation by Chandan K. Mozumder.

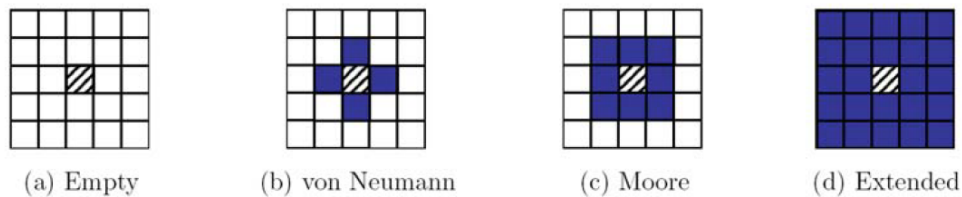


Figure 14: CA neighborhoods where (a) $\hat{N} = 0$, (b) $\hat{N} = 4$, (c) $\hat{N} = 8$, (d) $\hat{N} = 24$ [24]

Furthermore, Hao Chen et al. have performed a sensitivity analysis on a car door panel prior to the optimisation [6]. The sensitivity of the door modal frequency to the thickness of the door panel has been evaluated to study the influence of the design variables on structural performance, to find the most sensitive parts and reduce the number of design variables. The primary design variables in this study are the different parts of the door panel, such as the right or left inner panel and the window-frame vertical-reinforcing panel.

2.7.2 Adding rigidity

Structures with supporting ribs are widely adopted in many engineering fields. The stiffness is increased by adding supporting ribs on the main plate or shell. In order to get the most efficient stiffness for the ribs, their locations and dimensions are critical [18]. In [20], it is shown that the number of ribs also plays an important role in terms of the mechanical performance. Supporting ribs on shell structures have both good mechanical and geometrical properties. Ribs do not take up much space and utilise the bending characteristics, indicating better stability and avoiding stress concentrations.

The rib locations are generally constrained due to manufacturing limitation. Previous studies have shown that the rib locations can be determined by investigating the stress field [20] or by performing a topology optimisation [4] [19]. The dimensions of the ribs can be determined with topology optimisation [19] and the number of ribs can be found by analysing the strain energy increment that changes when ribs are added [20].

In [35], a parameter study was performed on how the width, length and height of ribs contributed to the overall stiffness. The results showed that increasing the length and height of the ribs were more effective than increasing the width.

3 Methodology

The model is divided into a grid of patches and a sensitivity analysis is performed to study the effects on the objectives. The most sensitive patches are thereafter refined whereas the nonsensitive patches are ignored in the further steps. The model with the refined patches is used for the topometry optimisation in several stages. This is an iterative process with the goal of finding an optimal rib pattern for the model. The sensitivity analysis and topometry optimisation are performed in *modeFRONTIER*. The methodology is applied on two models in this thesis work, configuration 3 and the side door. The first one was used to develop the methodology. Configuration 3 can be seen in Fig. 15a the side door in Fig. 15b.

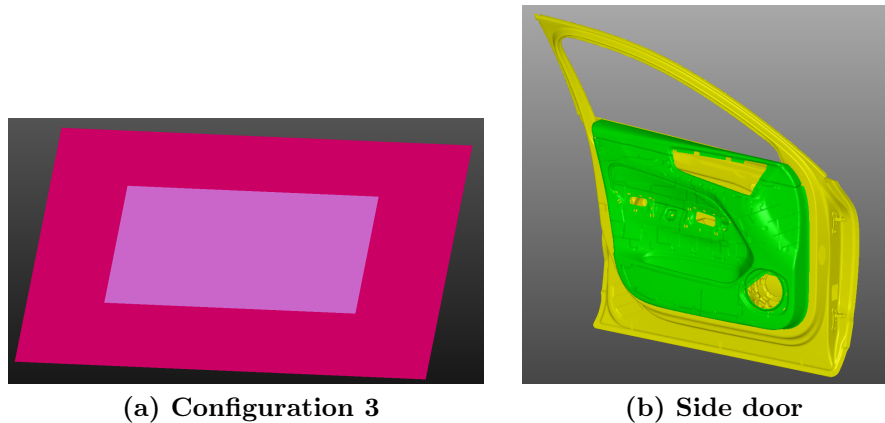


Figure 15: Models used in the thesis work

3.1 Optimisation problem

The mathematical formulation for the single disciplinary optimisations and the multi-disciplinary optimisation are formulated as stated below.

3.1.1 Geometric variation

Objectives: Minimise six sigma value (variation), minimise mean shift value (deviation)

Design variables: Coordinates for the center point of the patches

Constraints: Minimum thickness, number of input patches, mass

3.1.2 Dynamic response

Objectives: Minimise resonance risk, minimise mode shape dissimilarity

Design variables: Coordinates for the center point of the patches

Constraints: Minimum thickness, number of input patches, mass

3.1.3 Multi-Disciplinary Optimisation

Objectives: Minimise geometric variation (RD&T), minimise dynamic response (NASTRAN)

Design variables: Coordinates for the center point of the patches

Constraints: Minimum thickness, number of input patches, mass, proximity of thickened patches

3.1.4 Weighting of objectives

To make sure that all objectives are equally important for the sensitivity analysis and the optimisation, it is important to have a correct weighting between the objectives. The resonance risk and mode shape similarity number needs to be compared and weighted to give a fair representation of the objective for minimising the dynamic response, i.e. the NASTRAN objective. This also applies to the six sigma value and the mean shift value when minimising the geometric variation, referred to as the RD&T objective.

A DOE with 60 ULH generated designs is run to determine the weighting of the NASTRAN and RD&T objectives for a model. To find the weightings, the thickness of the patches are used as input design variables with two levels. The low level is equivalent to the original thickness and the high level is 1/3 larger.

The mean of each objective value is calculated and the weighting factor is the ratio between these two. The final weightings for the different models can be seen in Table 1, where the displayed factors are multiplied with the mean shift value and the mode shape similarity for the RD&T and NASTRAN objective, respectively.

Model	Weighting RD&T objective	Weighting NASTRAN objective
Configuration 3	19	5
Side door	79	86

Table 1: Weighting of objectives

3.2 Sensitivity analysis

Instead of optimising the whole part of the model directly, a sensitivity analysis is performed to identify the areas most sensitive to variation in thickness. These areas are defined as patches and are created by dividing the model into a grid pattern, as described in the modelling section.

The thickness of the patches are taken as the design variables in the sensitivity analysis. The design variables t_p , where $p = 1, 2, 3, \dots, n$ and n is the total number of patches, are numbered from left to right, top to bottom. The sensitivity of each patch is evaluated by studying the NASTRAN and RD&T objective values.

The thickness of the patches are allowed to have a value at two levels. Furthermore, no constraints are set in the sensitivity analysis.

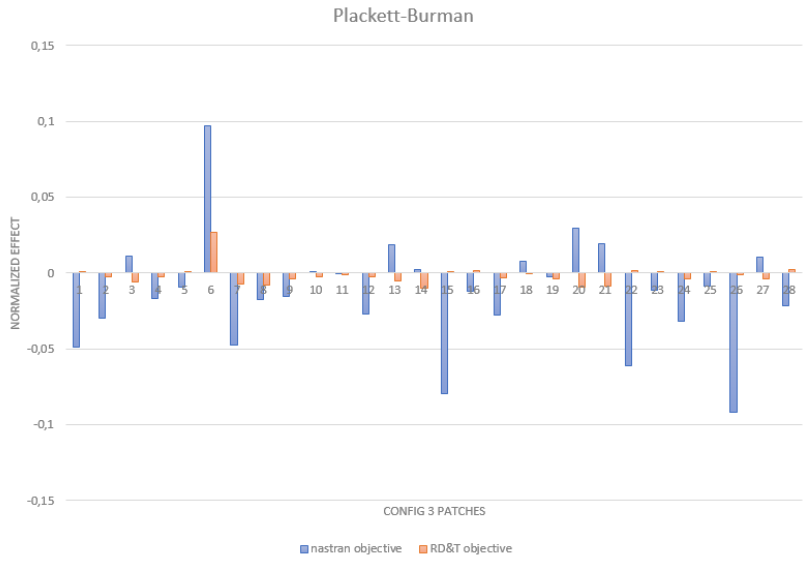
3.2.1 Evaluating Analysis Methods

Configuration 3, the configuration most similar to the side door panel, is used to determine which method to use in the sensitivity analysis. Different DOE tables with ISF designs where multiple design variables had different thicknesses in each design, led to inconsistent results and large errors. The R-squared values were especially low for the NASTRAN objective. The following parameters were altered, one at a time, to find a solution to this problem - additional levels of the

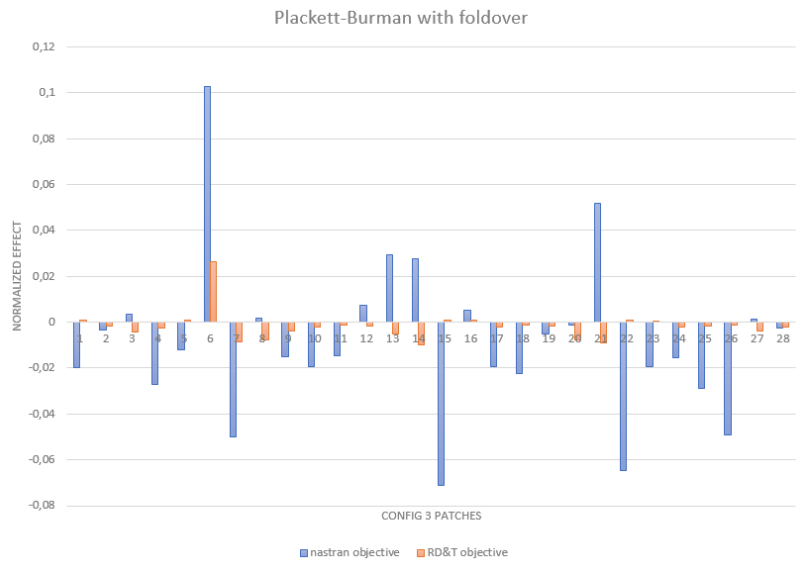
design variables, increased and decreased steps of the design variables, lower and higher maximum and minimum thickness, increased number of designs and altering different number of design variables in each design and in different patterns. However, results were consistent only when changing one variable at a time in each design, i.e. interactions were not taken into account. It was concluded that the system was sensitive and the results were dependent on how the DOE table was generated.

Factorial designs were considered and due to the large number of input variables, using a fractional factorial design would save computational time and cost by excluding several interactions. A Plackett-Burman design with foldover is therefore used. By adding a foldover, accuracy is increased and at least two-factor interactions are considered. The system is also less sensitive when accounting for less interactions. Whether a stable system with less evaluated interactions is more relevant than an unstable system with more evaluated interactions, is debatable. However, the choice of algorithm is based on the time inefficiency of running a full factorial design and the fact that the sensitivity analysis is mainly performed as a screening experiment.

Fig. 16 shows, for configuration 3, the difference between a Plackett-Burman design with and without foldover. The vertical axis represents the normalised effect of the patches and the patch numbers are represented on the horizontal axis. The low level thickness is 3 mm (original thickness) and the high level thickness is 4 mm (+33%). Most of the design variables with major effects in the Plackett-Burman design are also seen in the Plackett-Burman with foldover. However, it can also be seen that there are some differences in the predicted effects.



(a) Plackett-Burman



(b) Plackett-Burman with foldover

Figure 16: Normalised effect for design variables (patches) in configuration 3

3.2.2 Identifying relevant design variables

The influence of design variable X on an objective value is determined by the effect E_x and defined according to [11] as

$$E_X = Mean_+ - Mean_- \quad (7a)$$

$$Mean_+ = \text{mean of the objective value at the higher level} \quad (7b)$$

$$Mean_- = \text{mean of the objective value at the lower level} \quad (7c)$$

The effect is normalised with the nominal objective value where all design variables are at low level. This is done by subtracting and dividing the individual terms in Eq. 7a with the nominal objective value, respectively. To be able to compare the effect of the different objective values, one has to further normalise these effects with the mean of the previous normalised effects. The baseline is however, kept as the nominal value.

The design variables, i.e. the patches, that have largest effects on the objectives are selected and refined to smaller patches while the patches with little or no effects on the objectives are excluded. When refining to smaller patches, the elements in the vicinity of the boundaries of the patches are included to account for possible boundary effects.

The important design variables are determined by comparing the effect with a reference value, which is calculated as the mean of the latter negative normalised effects. For the design variables with positive effects on both objective values, one can conclude that these design variables should be kept at a low level to minimise the objective values. Thus, are these design variables not included in the optimisation.

A design variable is considered important if the normalised effect exceeds the reference value. In cases where one of the normalised effects is positive and the other negative, the design variable is of importance if one of the effects is significantly negative and the ratio of the positive effect to the negative effect is very small. This is evaluated with an additional criteria where the design variable is important if the positive effect is equal to or smaller than 10% of the

significantly negative effect.

The normalised effects and the patches in the sensitivity analysis for different models can be seen in Fig. 17, 18, 19 and 20. The results are shown in Table 2.

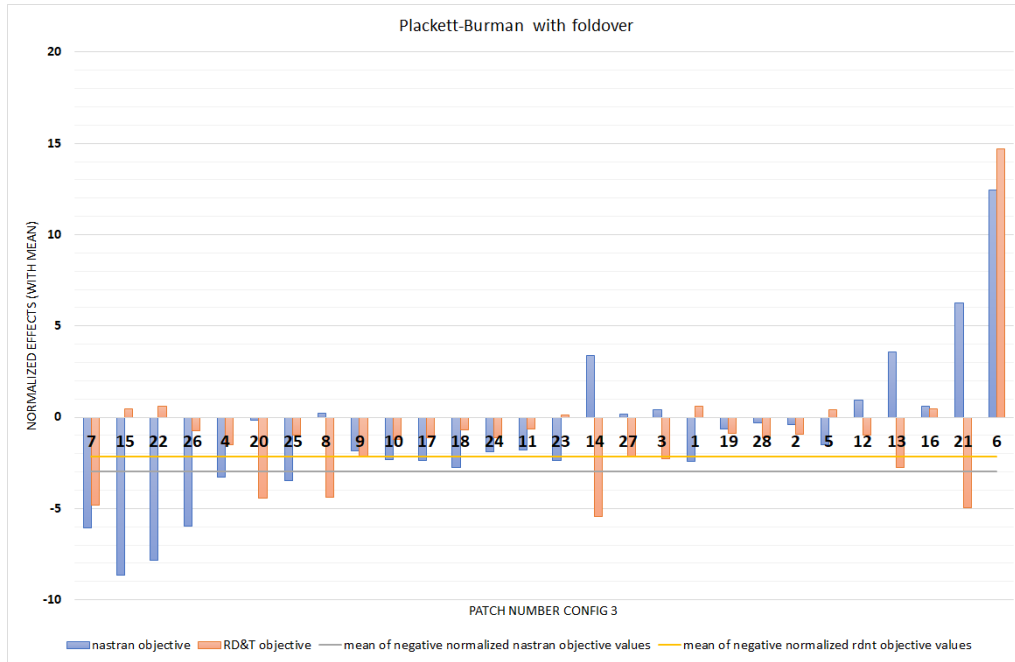


Figure 17: Sensitivity analysis for configuration 3

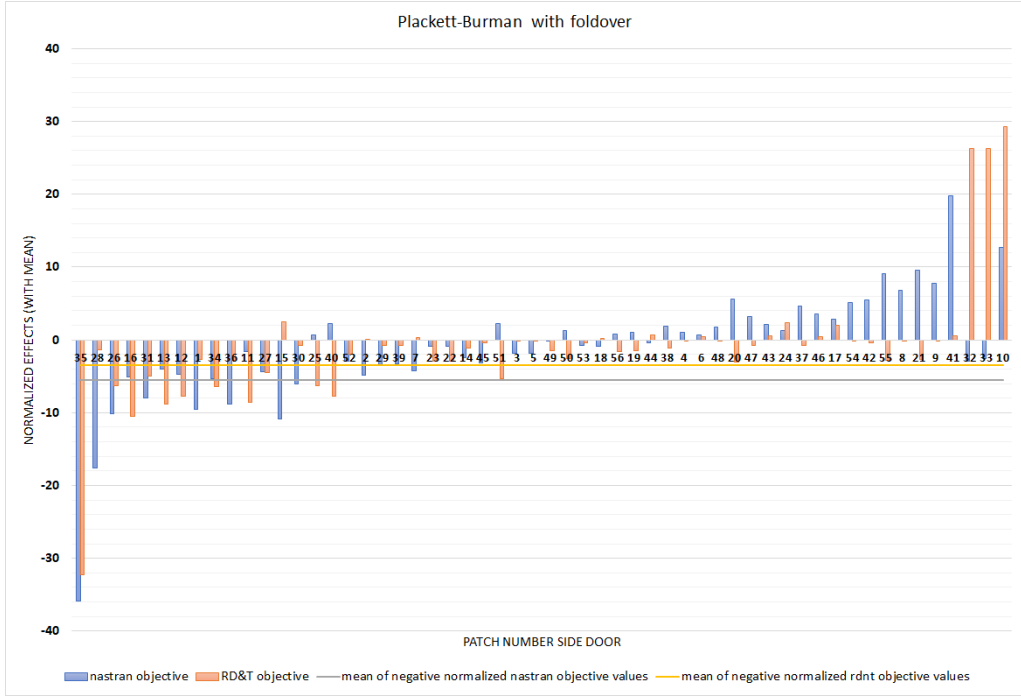


Figure 18: Sensitivity analysis for the side door

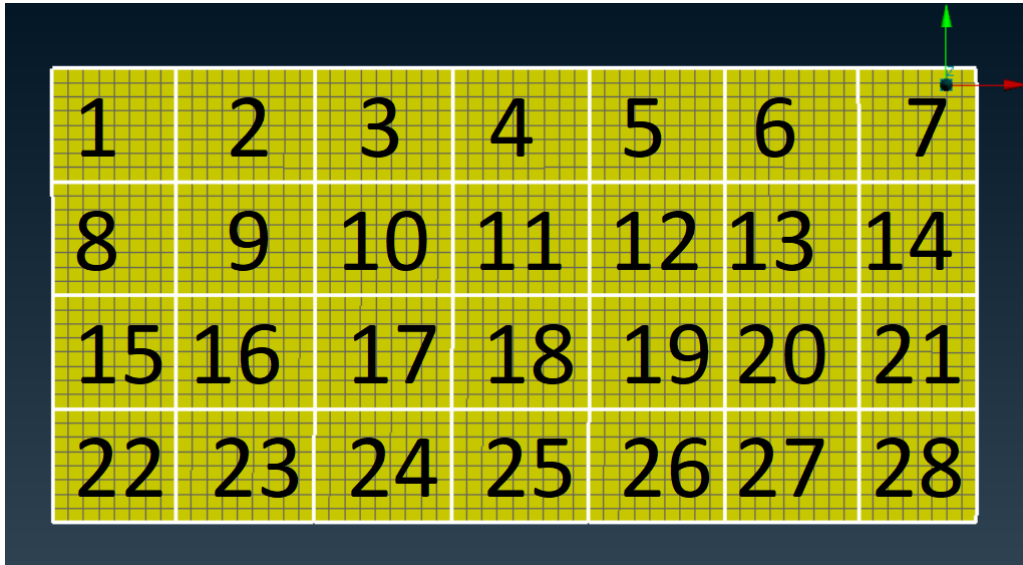


Figure 19: Patch numbers for the sensitivity analysis of configuration 3

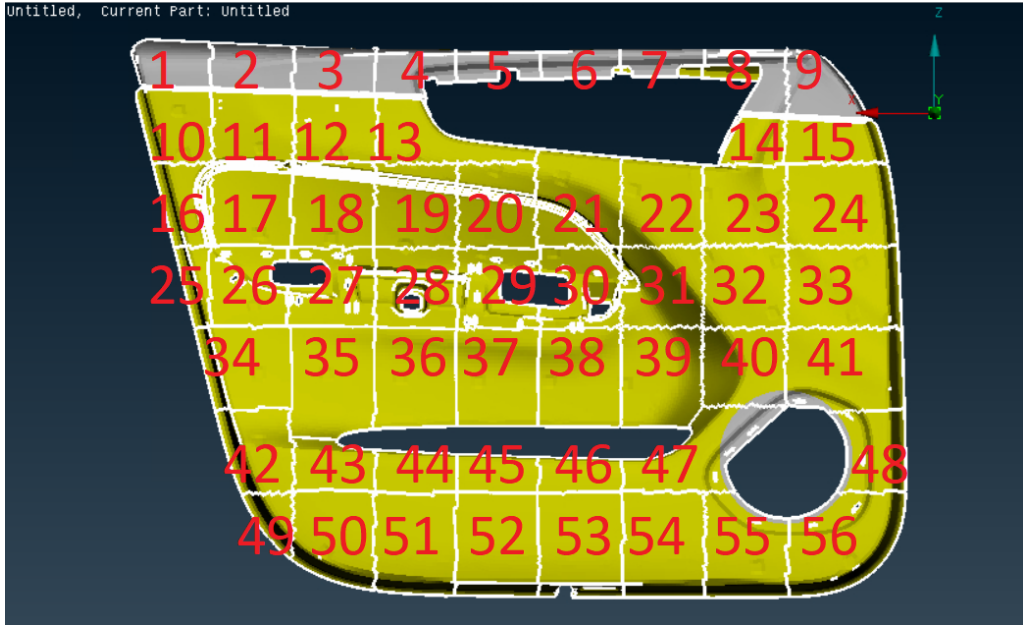


Figure 20: Patch numbers for the sensitivity analysis of the side door

Model	Low level (mm)	High level (mm)	Number of total patches	Important patches
Configuration 3	3	4	28	4, 7, 8, 15, 20, 22, 25, 26
Side door	1.8	2.4	56	1, 11, 12, 13, 16, 26, 27, 28, 30, 31, 34, 35, 36

Table 2: Data and results from the sensitivity analysis

3.3 First Optimisation Stage

The sensitivity analysis and refinement of the patches in ANSA (see modelling section), is followed by the first optimisation stage. To find the optimal design, the optimisation is divided into several stages where a pattern of added thicknesses is gradually formed stage by stage. The reasons for dividing the optimisation into multiple stages are to avoid unfeasible designs caused by the proximity constraint and to enable the possibility for patches to be thickened more than once if they require even more stiffness.

The optimisation method is a MOGA-II with an initial DOE generation. Each design in the optimisation has a number of inputs that varies between models, where one input represents one thickened patch. In the end, the design candidate with the best result on the Pareto front is selected and its patches are permanently thickened in the model. This is repeated in several optimisation stages and it is possible for one patch to be thickened in several stages, however it can only be thickened once in the same stage. In Table 6, the number of input patches, the thickness increase in each stage and the total number of optimisation stages are presented for each model. The number of input patches and the number of optimisation stages determines how many patches that will be thickened in the final stage. A summary of the workflow for the optimisation can be seen in Fig. 21.

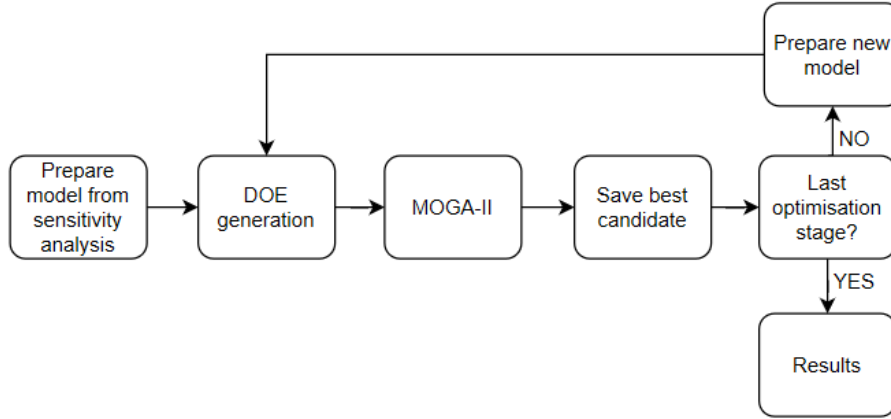


Figure 21: Optimisation workflow

3.3.1 Property identification number

The property identification numbers (PID) for the optimisation stages are based on the coordinates of a patch, similarly to the sensitivity analysis. It has the same format as the fasteners - NNXXYY, where NN is the part number and XX and YY represent the center coordinate for the patch in the x- and y-direction, respectively.

Since only some sections of the model are optimised, all coordinates are not represented by PIDs in the model. This creates a problem when having continuous variables representing the coordinates as input variables in the optimisation, since many designs generated by MOGA will be unfeasible. A constraint could be set to avoid running the unfeasible designs. This was tested, but resulted in too many designs that were omitted, which made the optimisation results unusable.

In order to solve this problem, the input variables are changed to be continuous from 1 to the number of patches with the stepping set to 1. Each value represent a specific patch and is translated to a PID by going through the PSHELL properties for the refined configuration. This ensures that no unfeasible designs are created by inputting nonexistent PIDs. The PSHELL properties are further explained the modelling section.

3.3.2 Modified Incremental Space Filler

ISF is used to ensure uniform distribution of the designs. When creating a DOE population that has design constraints, the limitations of modeFRONTIER's built-in incremental space filler function can make it difficult to create enough feasible designs.

To solve this problem, MATLAB is used to create a modified ISF that generates an evenly distributed population without violating any constraints. The MATLAB script needs the user to specify the population size and the total number of patches in the model.

The modified ISF starts by randomly assigning the input variables with values within the total number of patches. If this design does not violate any constraints it is saved to the DOE generation, otherwise it is randomly generated again until it is feasible. The constraints to be met are that the input values must be in a sorted order, they cannot be equal to each other and there cannot be any repeated designs.

To make sure that the input variables are evenly distributed, the number of occurrences for each variable is counted and compared to a maximum occurrence number. This number is also set as a constraint when generating the new designs. The maximum occurrence limit for each patch is formulated as

$$\text{max occurrence} = \frac{\text{number of input variables} \times \text{number of designs}}{\text{total number of patches}} \quad (8)$$

The DOE table is outputted as an Excel file which can be used in modeFRONTIER as the initial population for the MOGA-II optimisation.

3.3.3 Initial design of experiments size

According to [9], the initial training dataset can generally be calculated as Eq. 9.

$$DOE_{size} = 2 \times \text{number of input variables} \times \text{number of objectives} \quad (9)$$

Since the number given by this equation is just a recommended population size, it is just used as an approximation for the size of a population in an optimisation stage. The actual size is dependent on how well the created MATLAB script generates a well distributed population, which in turn is dependent on the total number of patches and the number of input variables. The size of the initial DOE population for each optimisation stage for configuration 3 and the side door are shown in Tables 3 and 4, respectively.

	DOE size
Stage 1	26
Stage 2	27
Stage 3	26
Stage 4	28

Table 3: DOE size for the optimisation stages for configuration 3. DOE size = 28 according to Eq. 9

	DOE size
Stage 1	44
Stage 2	40

Table 4: DOE size for the optimisation stages for the side door. DOE size = 44 according to Eq. 9

3.3.4 Number of generations

The number of generations is set such that the solution can converge, i.e. the optimal designs in the latter generations should be identical. To reach convergence, 50-150 generations are set in an optimisation stage, but the optimisation can be stopped if convergence is reached before the last generation. Moreover, unfeasible designs may be a problem in the next optimisation stages since the risk of violating constraints increases. Thus, is it also important to have a large number of generations and to ensure that the solution converges.

3.3.5 Selection of the best candidate on the Pareto front

The best candidate is manually chosen from the Pareto front. The goal when choosing the best candidate is primarily to minimise both objectives as much as possible without prioritising one more than the other. The patches from this best candidate are to be permanently thickened with a predetermined value for the further optimisation stages.

3.4 Further Optimisation Stages

The further optimisation stages are similar to the first one, however a few more things need to be considered since the model should be changed based on the previous results. The first part of this is creating a new model in ANSA. The old one could be used but in order to decrease the number of unfeasible designs, the patches that are considered as too far away from the already thickened ones are removed from the model. If they should be considered close again in future optimisation stages, they are brought back for consideration. This process is described further in the modelling section.

The thickened patches from the previous optimisation stages need to be permanently thickened. This includes defining a new thickness for them for the next optimisation stage. The number of times a patch can be thickened is only limited by the number of optimisation stages.

3.5 Constraints

Some constraints need to be defined and implemented in order for the applied method to work as intended. This section describes the constraints, how they work and when they are applied.

3.5.1 Sorting

The sorting constraint sorts the input number that represents a patch, ranging from 1 to the number of patches, in ascending order. Since the order of the patches is irrelevant and gives equivalent results, sorting the input number results in avoiding the evaluation of duplicate designs. The optimisation is therefore more efficient since computational time is reduced.

3.5.2 Proximity

Since the idea is to replace the optimal thickened areas with ribs, one has to consider how these optimal thickened areas are distributed. A rib is a continuous construction and it is therefore critical to introduce a constraint that considers the proximity of the optimal thickened patches to make sure that the pattern is suitable for being replaced with ribs.

A design violates the proximity constraint if several patches are located far away from the patches that have been a part of an optimal design in previous optimisation stages. Two patches are considered far from each other if the distance between their imaginary rectangular center points exceeds a threshold value. The threshold value is mathematically defined as

$$d = \sqrt{(x_p - x)^2 + (y_p - y)^2} \quad (10)$$

where x and y are the coordinates for the imaginary rectangular center point of a patch and index p indicates the current patch that is evaluated against the patches in optimal design from previous optimisation stage.

In this case, the threshold value is estimated such that the first neighboring patches are considered to be close. The constraints in the optimisation algorithm are treated as penalising objectives, thus are the patches in the second neighborhood, considered as far, penalised proportionally to the estimated constraint violation if there are more than n patches in the second neighborhood. The value of n is chosen based on the number of input patches and can be seen in Table 5.

Model	n
Configuration 3	2
Side door	6

Table 5: n -values for the different geometries

The proximity constraint is not considered in the sensitivity analysis nor in the first optimisation stage since the constraint is formed such that the optimal designs forms a pattern of thickened patches. It therefore requires already thickened patches in order to be applied.

The idea behind this constraint is taken from a previous study from Chandan K. Mozumder where the HCA algorithm has been used. However, instead of updating the state of a patch based on its neighborhood, the neighboring elements of a patch are considered as acceptable candidates.

3.5.3 Mass

The mass of the model is an important aspect considering efficiency and cost. A mass constraint is therefore introduced where a maximum percentage of the total increase in mass is set. In this thesis, the maximum increase in mass is set to 5%, which is equivalent to a maximum of 5% increase in thickness. To determine the number of input patches (a), number of optimisation stages (b) and the increase in thickness (mm) per optimisation stage (c), one has to fulfill the expressions in Eq. 11, related to the mass constraint.

$$\frac{ab(\text{low}+c) + \text{low}(\text{number of patches}-ab)}{\text{low} \times \text{number of patches}} \leq 1.05$$

$$\text{low} + bc = \text{final maximum thickness of a patch} \quad (11)$$

a, b reasonable values

low is the low level thickness of the patches and *number of patches* is equivalent to the grid size after refinement. The final maximum thickness of a patch is the

accumulated final thickness of a patch if that patch is thickened up in every optimisation stage. Furthermore, a and b are selected such that patches of different thicknesses are distinguishable and shows a clear pattern of the areas that need to be thickened up. The values of a , b and c are seen in table 6

Model	a	b	c (mm)	low (mm)	number of patches	final maximum thickness of a patch (mm)	increase in weight (%)
Configuration 3	7	4	0.5	3	96	5	4.86
Side door	11	2	0.3	1.8	158	2.4	2.32

Table 6: Estimated a , b and c according to Eq. 11

3.6 Flow charts

The flow chart in Fig. 22 shows the general approach in this thesis work. The DOE is performed according to Fig. 23.

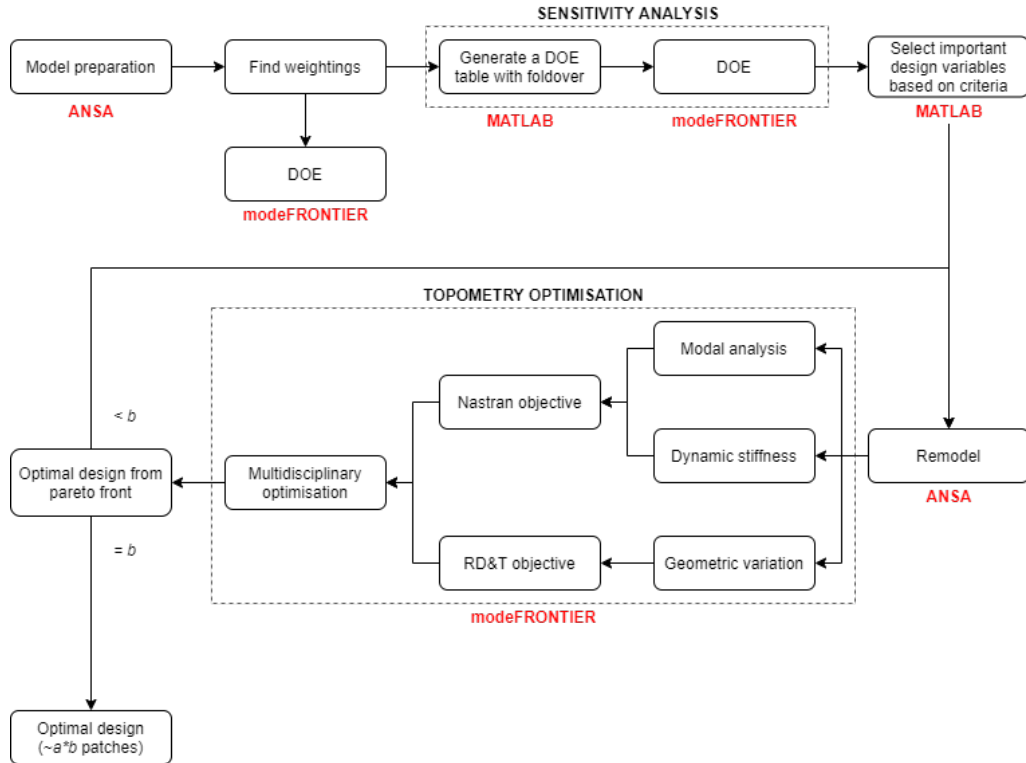


Figure 22: Flow chart of the methodology, a =number of input patches and b =number of optimisation stages

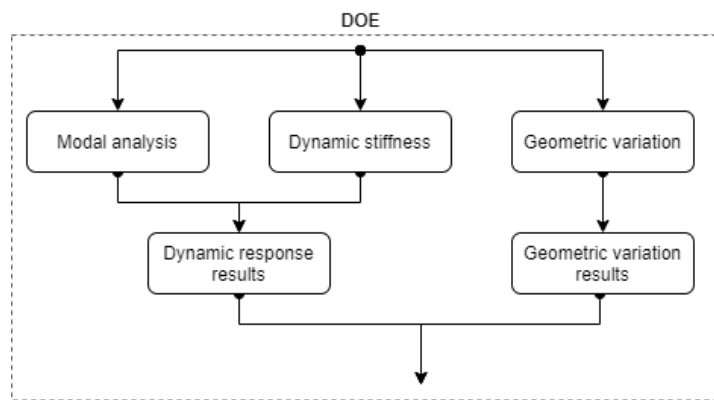


Figure 23: Flow chart of a DOE analysis

4 Modelling

This chapter describes which and how assemblies of a car and simplified geometries are modelled. The patches of the models are created and further refined in *ANSA*. The refined models are then exported for use in *RD&T* and *modeFRONTIER*.

4.1 Model selection

The geometries used in this thesis are based on previous projects at VCC where they have been identified as assemblies of a car that are prone to squeak and rattle. One simplified geometry, configuration 3, and one full model of a side door have been studied. The side door is the corresponding component of configuration 3. The mesh of the geometries are also provided. Figs. 22 and 23 shows the simplified geometry and the full model of the side door, respectively.

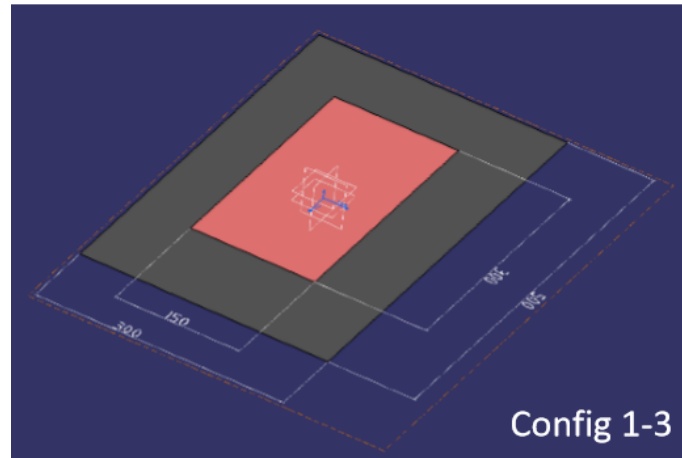


Figure 24: Configuration 3, simplified geometry

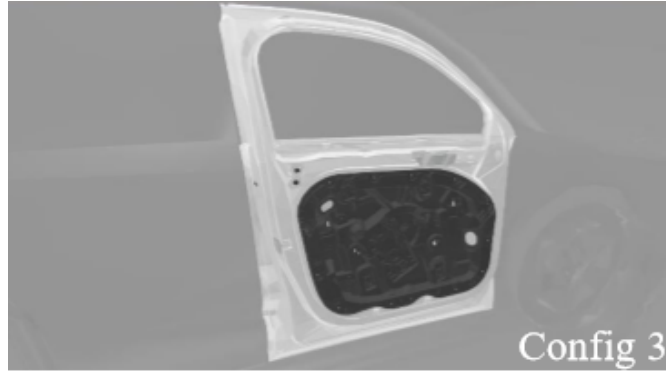


Figure 25: Side door, full model

4.2 CBUSH

A CBUSH element is a generalised spring and damper element that can be used with coincident nodes. In NASTRAN, it is defined between two nodes using the CBUSH element card and the PBUSH property card. The PBUSH properties are defined for each of the six degrees of freedom and can have separate stiffness values, damping coefficients and structural damping coefficients in all these directions [2].

In this work, CBUSH elements are distributed across the models at all possible locations for fasteners between the two parts. The PBUSH properties are then edited to determine which fasteners are active and in which direction.

4.3 PSHELL

The patches are created with shell elements in ANSA. The shell element property defines the membrane, bending and transverse properties for each shell element [30]. In this thesis, each shell element are given a PID and the thickness is optimised in modeFRONTIER and updated accordingly to each design. The remaining properties are kept as the default values.

4.4 Modified fasteners

The positions of the fasteners in the models have been optimised in the previous thesis work. It resulted in a number of fasteners constraining the models in the normal direction, some of which also constrain the configuration in the planar directions [16].

Using more than two planar fasteners or using two fasteners directed in both planar directions on parts that are flat makes the assembly over-constrained. Over-constraining leads to complicated and time consuming simulations in RD&T. In order to reduce the time it takes to run each design in RD&T, the planar fasteners needs to be reconfigured with the objective of finding a positioning configuration with similar results as the optimised one but with a shorter simulation time.

In order to evaluate the influence of the positioning and directions of the planar fastener on the RD&T run time as well as the NASTRAN and RD&T objectives, simulations are performed on configuration 3. The optimised positioning of the fasteners for configuration 3 can be seen in Fig. 26.

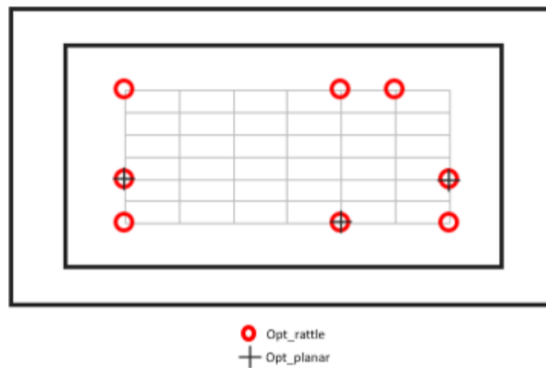


Figure 26: Optimised fastener positions [16]

To improve the positioning of the planar fasteners a version of the 3-2-1 locating principle called N-2-1 was used. The "N" in this case is already represented by the fasteners in the normal directions, leaving the "2" and "1" to be decided. According to [12], the points should be positioned as far from each other as pos-

sible. With this in consideration, the planar fasteners that are the furthest away from each other are kept and the others are eliminated. For configuration 3 this lead to the elimination of the planar fastener FP10504. The decision remaining to be made is to decide which of the X and Y directions that should be constrained twice and which of the fasteners that should constrain in two directions.

Even though the NASTRAN solver does not have the same problem with the planar fastener configuration, the CBUSH properties for the fasteners are changed to the same as in RD&T to maintain consistency. The weighting for the objectives that is used for the optimised model are used in this evaluation to make the results comparable. The results of the planar fastener evaluation are presented in Table 7. They are obtained by running one design for configuration 3 with thickness 3 mm for all patches.

Activated planar fasteners and directions	Value of NASTRAN objective	Value of RD&T objective	RD&T run time (s)	Total run time (s)
<i>FP10103 (X, Y)</i> <i>FP10504 (X, Y)</i> <i>FP10703 (X, Y)</i>	<i>2.4378E4</i>	<i>4.4105E1</i>	<i>574</i>	<i>582.538</i>
FP10103 (X, Y) FP10703 (X, Y)	2.5131E4	1.3227E1	213	223.484
FP10103 (X, Y) FP10703 (Y)	2.4387E4	5.5410E0	93	224.154
FP10103 (Y) FP10703 (X, Y)	2.4386E4	5.5409E0	93	241.898
FP10103 (X, Y) FP10703 (X)	2.4969E4	9.7731E0	213	232.052
FP10103 (X) FP10703 (X, Y)	2.4962E4	1.5117E1	213	229.491

Table 7: Value of the NASTRAN and RD&T objectives with different activated planar fasteners in different directions. The fasteners and values in italic and bold are the original fasteners activated in the optimal design in the previous VCC thesis work.

A few observations can be made from the simulation results in Table 3. The first one being that one run in RD&T takes around six times as long for three planar fasteners compared to the ones with the shortest run time. It can also be seen that the run time is much shorter when the fasteners are not directed towards each other. How the same set of directions are combined does not affect the run time.

When it comes to the objectives, the NASTRAN objective is almost unaffected by the variation of the planar fasteners, whereas the RD&T objective changes

greatly when changing the fasteners.

The fact that the total run time varies for those with the same RD&T run time is worth mentioning, however this is probably due to the variation of the server load for each run.

When setting up the planar fasteners in configuration 3 for the topometry optimisation, the great reduction in run time is considered as more important than the fact that the RD&T objective value differs from the optimised configuration. This decision is based on the fact that the aim of this work is to minimise the objectives rather than to achieve an absolute value. This also affects all designs in the same way so they can still be compared to each other.

Based on the results of this planar fastener evaluation, all models used in the topometry optimisation with over-constraining optimal fasteners, will only have two planar fasteners, one of which has two directions and the other one direction. These directions should not be directed towards each other since that prolongs the run time. The two fasteners to be kept are the two that are the furthest away from each other. The planar fastener with the lowest x-coordinate value will have two directions and the one with the highest x-coordinate value will have one. This decision is taken to have the same approach for all models.

Editing the fasteners in this way will have an effect on the results, as seen when comparing the results in Table 7. Since this thesis work mainly focuses on the development of the methodology rather than creating an optimal model, the changed behaviour caused by the fasteners is not a problem.

4.5 Configuration 3

Configuration 3 is a simplified assembly consisting of two parallel and coincident planes that are supposed to represent the inner and outer panels of a side door. Configuration 3 and the side door can be seen in Figs. 24 and 25, respectively.

For the side door, the outer part is made of mild steel and the inner part is made of Stamax 30YK270 (PPLGF30), which is a glass fiber reinforced polypropylene.

The topometry optimisation is only performed on the plastic part since it is easier to vary the thickness of a plastic part than a steel part because of their different production methods.

For the sensitivity analysis, configuration 3 was divided into 28 patches in a 7x4 grid pattern which can be seen in Fig. 27. The dimensions of the patches are 45x40 mm. However, the patches in the first and last columns are of size 40x40 mm. The patches were created in ANSA.

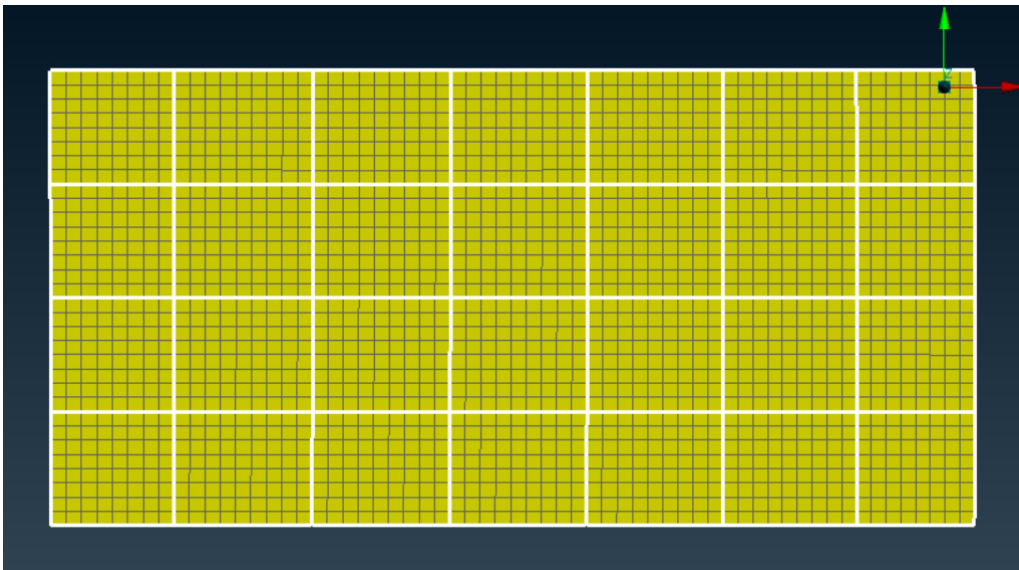


Figure 27: Initial distribution of patches for configuration 3

4.5.1 Fasteners

The optimisation of the fastener positions in configuration 3 from the previous thesis work resulted in eight fasteners in the normal direction and three in both planar directions [16]. These optimised fastener positions can be seen in figure 26.

As previously described, the two planar fasteners furthest apart should be kept when configuring the fasteners according to the N-2-1 locating principle. For

configuration 3, this results in the elimination of the planar fastener FP10504, keeping FP10103 in both planar directions and keeping FP10703 only in the Y-direction. The fasteners in the normal directions are kept in the optimisation for configuration 3. The two selected planar fasteners are marked with blue squares in Fig. 28. The one at the bottom right corner is the one with only one direction in y.

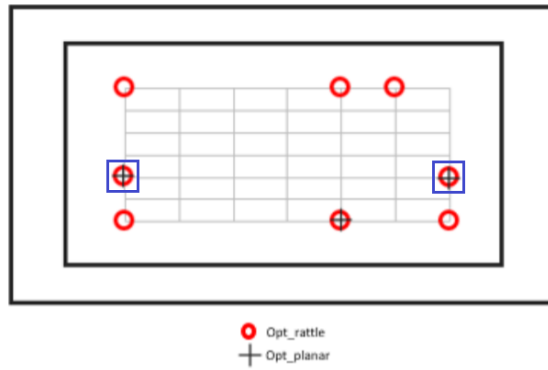


Figure 28: Fasteners used in the topometry optimisation for configuration 3 [16]

4.5.2 Refinement after Sensitivity analysis

The sensitivity analysis of configuration 3 led to 8 out of 28 patches being sensitive and important. The sensitive areas are depicted in Fig. 29 with white edges.

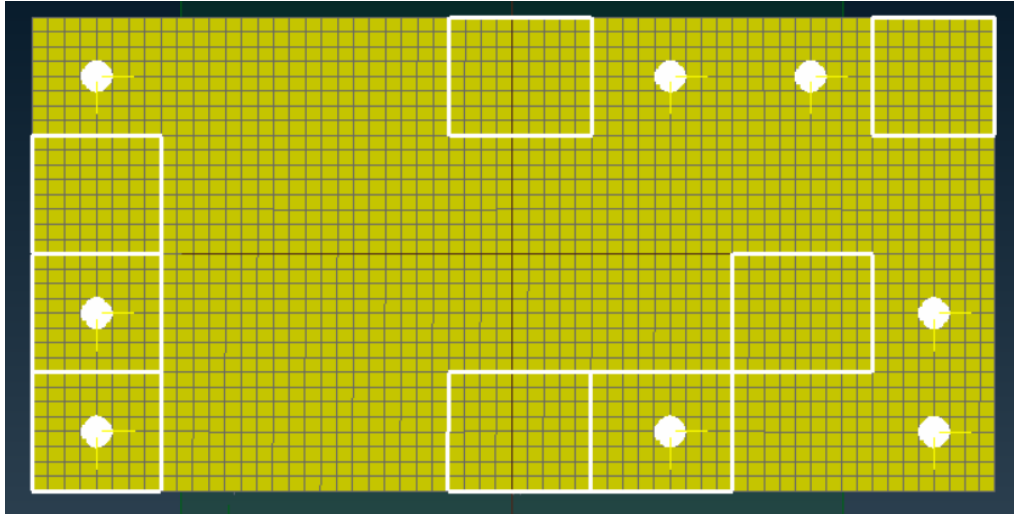


Figure 29: Identified areas from sensitivity analysis for configuration 3

The patches in Fig. 29 need to be refined for the first optimisation stage. The areas around the fasteners are also included in the refinement. The fasteners are depicted as white circles in Fig. 29. The reasoning behind this is that the areas around the fasteners should be important since that is where the load transfers and the effect of that might be overlooked because of the large size of the initial patches.

The refinement is done by first dividing the whole model into a finer grid and then removing the grid squares that are not part of the areas to be refined. The refined grid consists of 12x8 patches with as even dimensions as possible. The dimension of these patches are 25x20 mm. Due to the fact that the model is 61 elements wide, one column of squares is one element wider than the rest. The dimension of these patches are 30x20 mm. The refined version of configuration 3 with 52 patches can be seen in Fig. 30. The PIDs of the patches are based on their position in the 12x8 grid to make it possible to compare their proximity to each other.

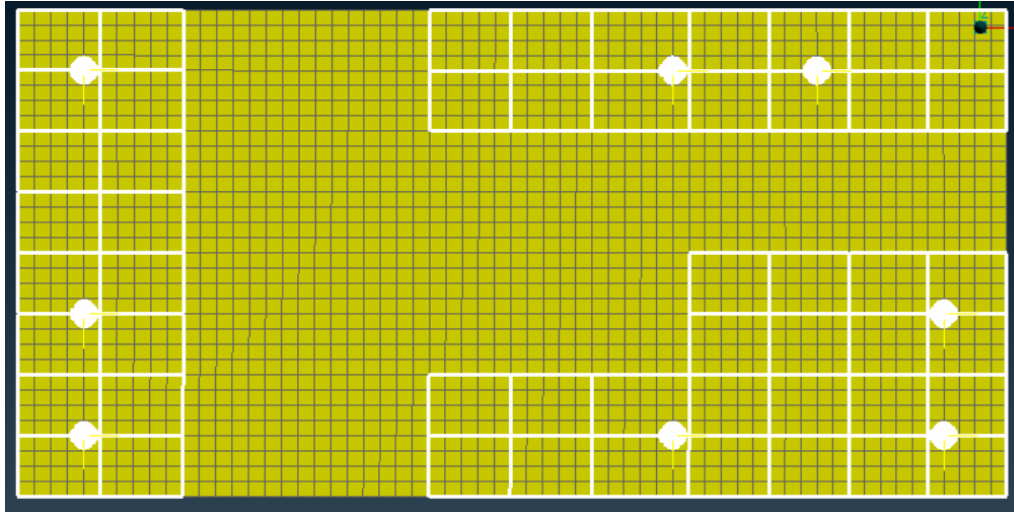


Figure 30: Refined areas for the first optimisation stage for configuration 3

4.5.3 Refinement after first optimisation stage

The thickened patches of the best candidate of the first optimisation run can be seen in Fig. 31 and their PIDs are presented in Table 8. Since the fasteners do not seem to be a large factor for which patches are thickened, they are not shown in the further figures until the final design is reached.

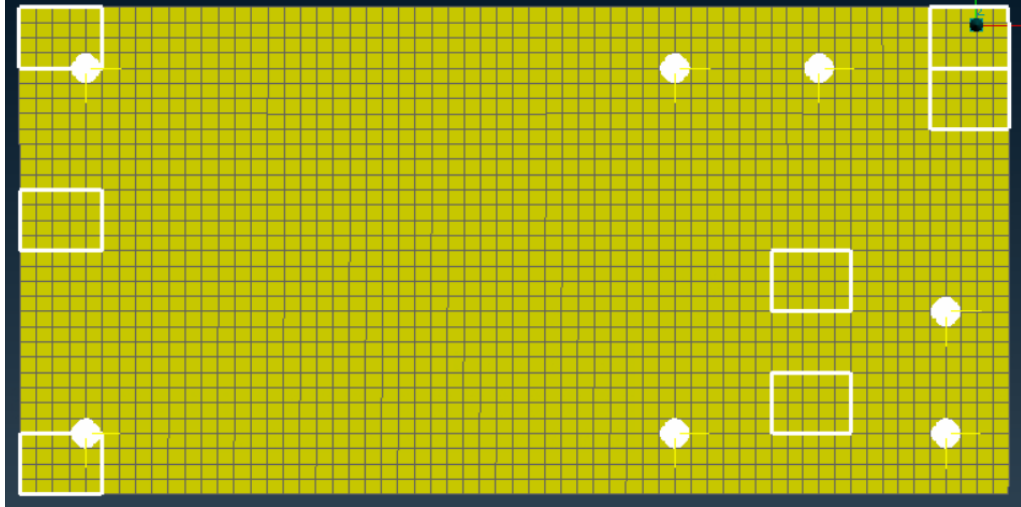


Figure 31: Thickened areas after the first optimisation stage for configuration 3

PID	100101	100104	100108	101005	101007	101201	101202
Thickness (mm)	3.5	3.5	3.5	3.5	3.5	3.5	3.5

Table 8: PIDs and their new thickness from the best design of the first optimisation stage

To reduce the number of unfeasible designs generated in the MATLAB script that creates the DOE table and thereby affects MOGA-II, the patches that are far away from all thickened patches are removed for the second optimisation. This reduced the number of patches from 52 to 37, see Fig. 32.

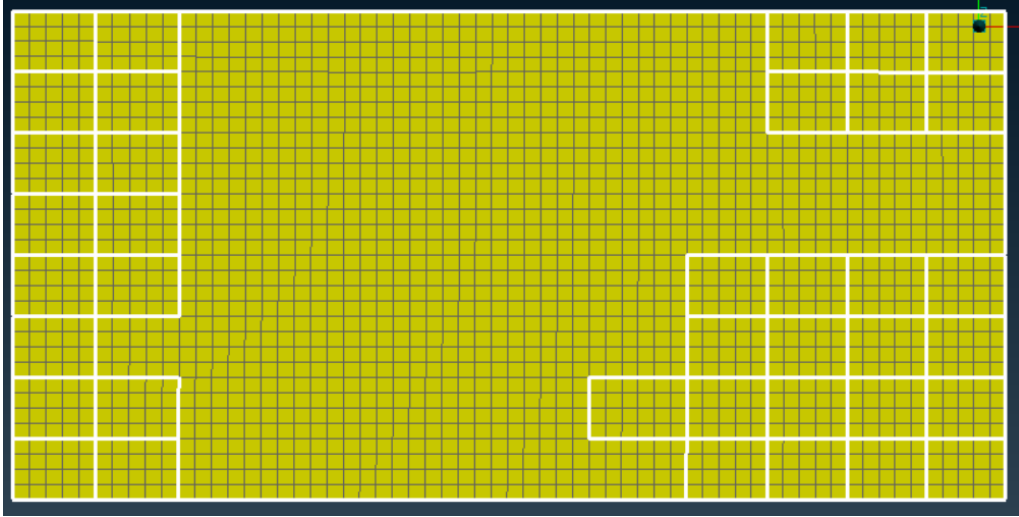


Figure 32: Available patches for the second optimisation run for configuration 3

4.5.4 Refinement after second optimisation stage

The new patches after the second optimisation are marked with red in Fig. 33. Their PIDs are presented in Table 9. The patch with PID 101202 was chosen in both the first and the second optimisation. The thickness of this patch is therefore 4 mm. The new addition of patches from the second optimisation results in a total of 12 thickened patches to 3.5 mm and one thickened to 4 mm, see Fig. 33.

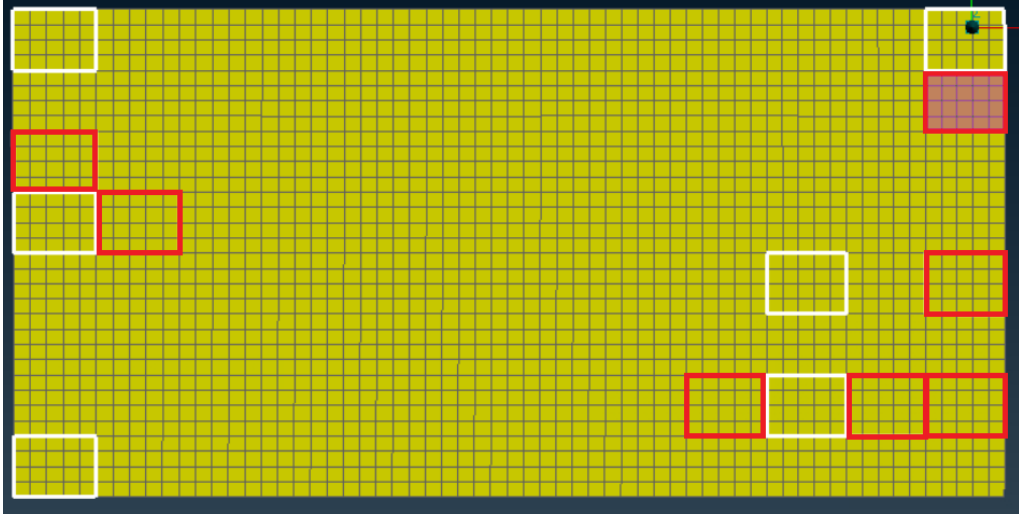


Figure 33: Thickened areas after the second optimisation stage for configuration 3. Patches from the current stage have red edges and the purple patches are 4 mm thick.

PID	100103	100204	100907	101107	101202	101205	101207
Thickness (mm)	3.5	3.5	3.5	3.5	4.0	3.5	3.5

Table 9: Added PIDs and their new thickness from the best design of the second optimisation stage

The new thickened patches creates the possibility for four more patches to be a part of a feasible design. With these added, the number of patches becomes 41, see Fig. 34.

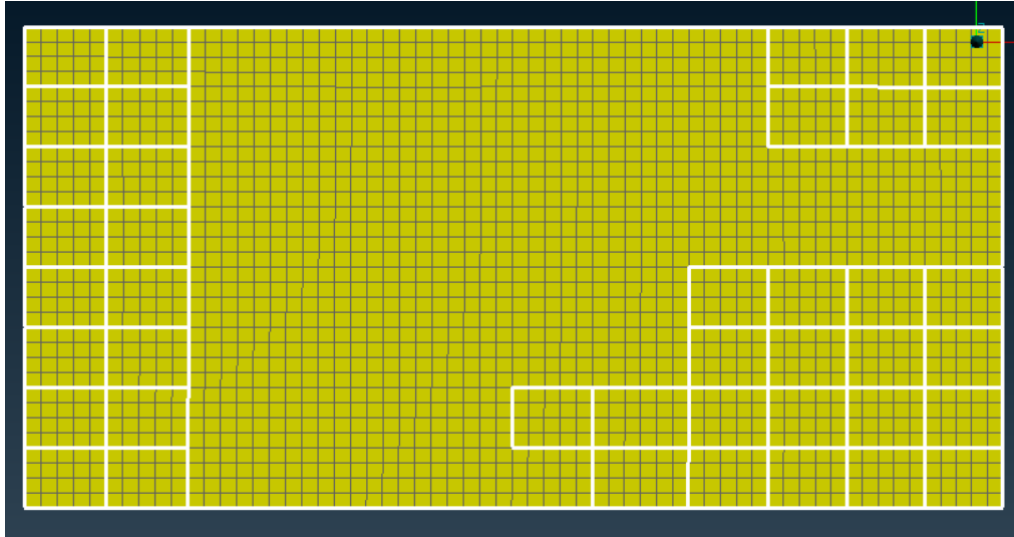


Figure 34: Available patches for the third optimisation stage for configuration 3

4.5.5 Refinement after third optimisation stage

The new patches after the third optimisation are marked with red edges in Fig. 35. Their PIDs are presented in Table 10. None of the patches from the previous stages had been thickened up again, resulting in a total of 19 thickened patches to 3.5 mm and one thickened to 4 mm, see Fig. 35.

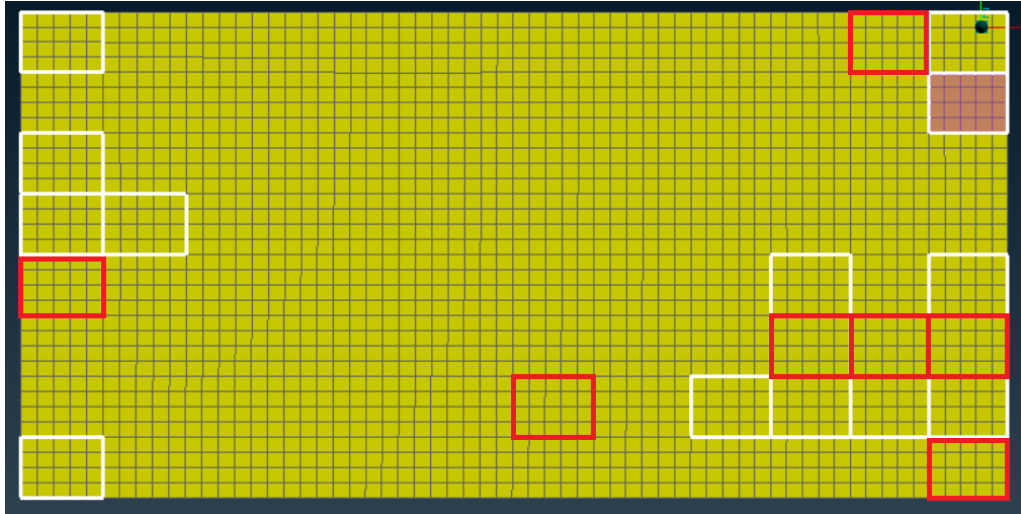


Figure 35: Thickened areas after the third optimisation stage for configuration 3. Patches from the current stage have red edges and the purple patches are 4 mm thick.

PID	100105	100707	101006	101101	101106	101206	101208
Thickness (mm)	3.5	3.5	3.5	3.5	3.5	3.5	3.5

Table 10: PIDs and their new thickness from the best design of the third optimisation stage

Once again, the new thickened patches creates the possibility for four more patches to be a part of a feasible design. This results in a new model with 45 patches, see Fig. 36.

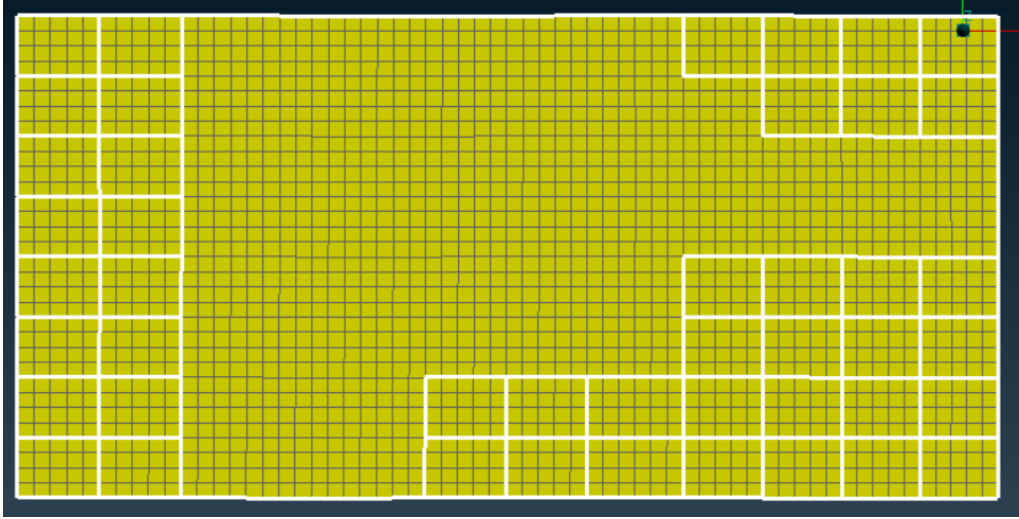
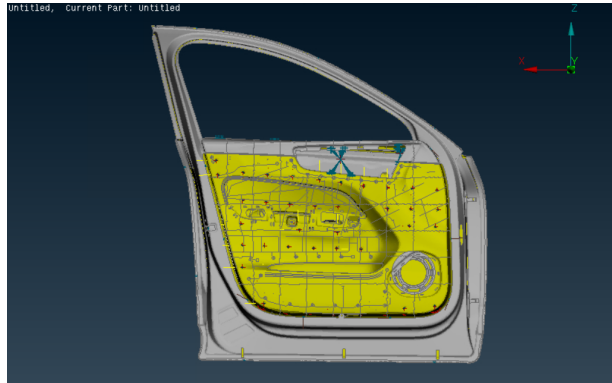


Figure 36: Available patches for the fourth optimisation stage for configuration 3

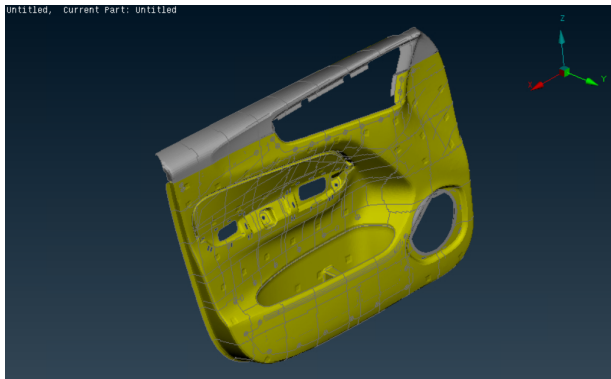
The fourth optimisation stage is the last stage for this configuration and there are therefore no further refinements of the model. The results from the fourth optimisation are presented in the results section.

4.6 Side door

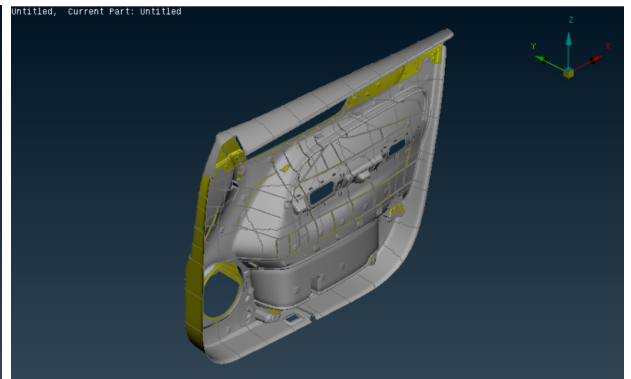
The side door model that is used is seen in Fig. 37a. Its main parts are the outer steel frame of the door and the inner door panel, where the latter is the part to be optimised. The inner door panel consists of two parts itself which are made of different materials. The largest part is made of natural fiber reinforced polypropylene, shown as yellow in Fig. 37b. The other part is made of an ABS plastic called Styrolution Terluran GP-22 and is the upper grey part of the inner door panel in Fig. 37b. Both parts on the inner door panel have the nominal thickness of 1.8 mm.



(a) Full model



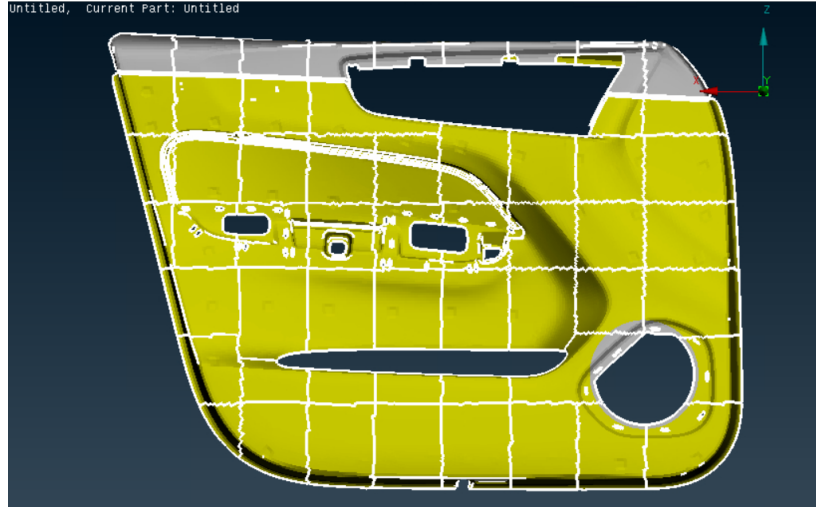
(b) Inner door panel, front view



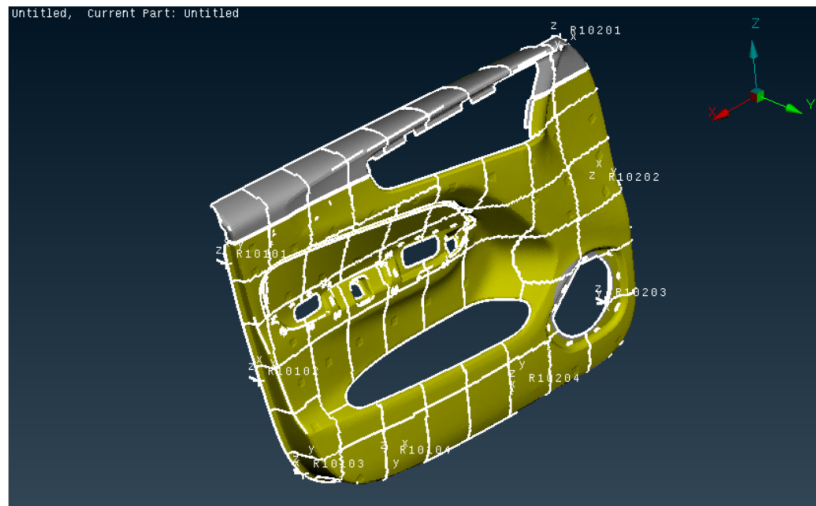
(c) Inner door panel, back view

Figure 37: ANSA model of the side door

For the initial sensitivity analysis, the inner door panel, consisting of the two parts in Fig. 38, is divided into 56 patches in a 9x7 grid. Each patch is of size 100x100 mm. When creating a grid pattern in ANSA, a few patches turned out to be quite small and are therefore added to the neighboring patch to reduce the number of design variables and save computational time. Furthermore, the patches are created to be as rectangular as possible and defined such that the two different materials of the inner door panel are separated.



(a) Front view



(b) Side view

Figure 38: Initial distribution of the patches in the side door

4.6.1 Fasteners

Previous thesis work have been done to optimise the position of the fasteners for the side door model. It resulted in ten fasteners in the normal direction, four of which also constrained the model in the two planar directions [16]. The optimised fasteners for the side door can be seen in Fig. 39.

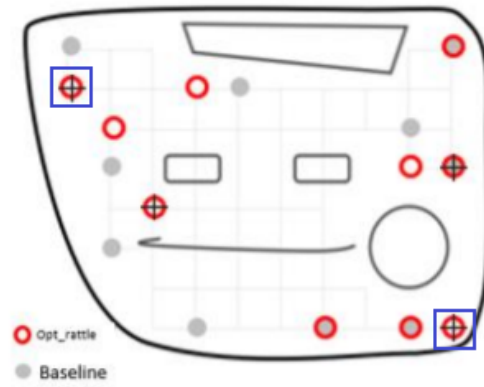


Figure 39: Optimal fasteners for side door

As mentioned in the section of modified fasteners in the methodology, too many planar fasteners in a flat model increases the risk of an over-constrained model. Even though the side door model is not as flat as the simplified configuration, the four planar fasteners still created problems and the model was not able to be analysed for geometric variation in RD&T with all of them being activated.

After testing different set ups with fewer fasteners, the decision fell on using the same approach as for configuration 3. This means using two planar fasteners, one in both planar directions and the other in only the y-direction. The two selected fasteners are 50102 and 51008, marked with blue squares in Fig. 39. The one at the bottom right corner is the one with only one direction in y. The reasoning behind selecting them is that they are far apart and they are both part of four of the five optimal designs found on the Pareto front from the previous thesis work that optimised the fastener positions [16].

4.6.2 Refinement after the sensitivity analysis

The sensitivity analysis of the side door identified 13 out of 56 patches as sensitive and important, marked out with white edges in Fig. 40.

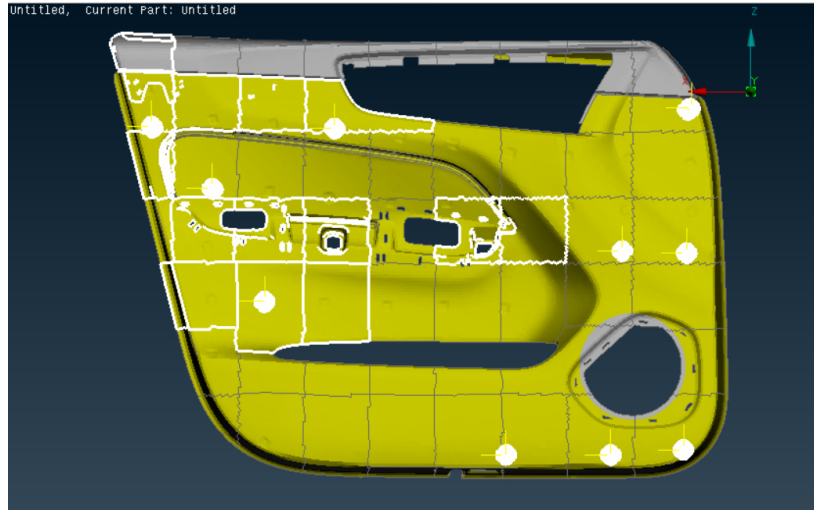


Figure 40: Identified areas from sensitivity analysis for the side door

The side door is refined by dividing the model into a finer grid pattern of size 15x12. To account for possible boundary effects, each patch is 60x60 mm and created to be slightly larger than half of one patch in the initial model. The patches are as evenly divided as possible, however some patches are bigger and less rectangular than others due to the shape of the model. The areas around the fasteners are also included in the refinement, similar to configuration 3. The total number of patches in the refined model is 158 but only 66 patches, covering the sensitive areas from the sensitivity analysis, are included in the first optimisation stage. The PIDs for the refined model are based on their imaginary rectangular center point and the model used for the first optimisation stage is seen in Fig. 41.

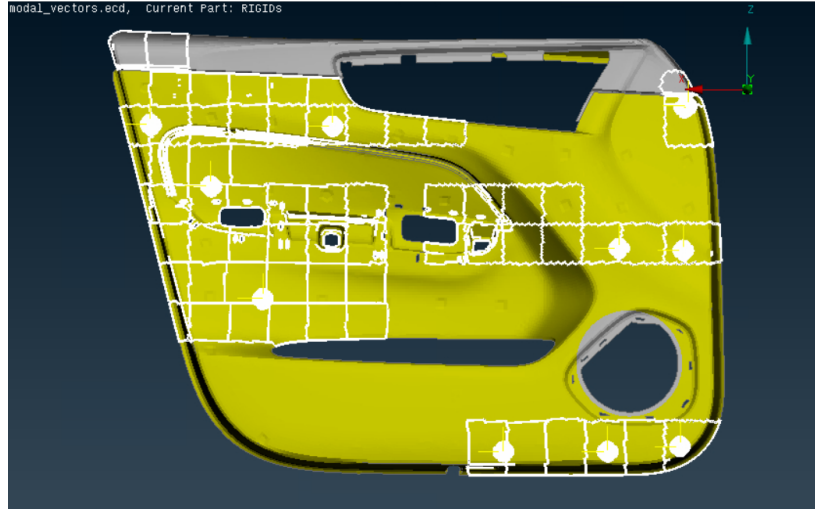


Figure 41: Refined areas for the first optimisation stage for the side door

4.6.3 Refinement after first optimisation stage

The thickened patches from the optimal design of the first optimisation stage for the side door can be seen in Fig. 42 and their PIDs are presented in Table 11.

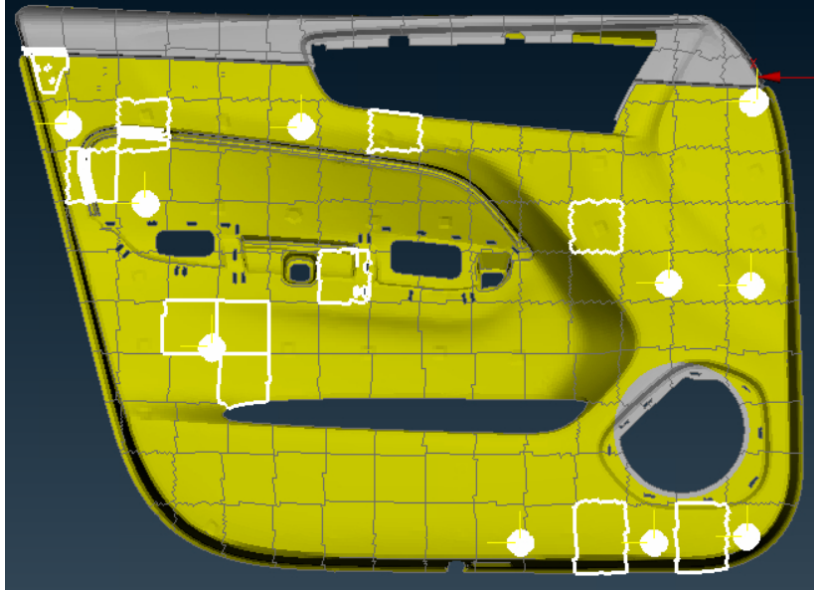


Figure 42: Thickened areas after the first optimisation stage for the side door

PID	Thickness (mm)
300102	2.1
300205	2.1
300304	2.1
300408	2.1
300508	2.1
300509	2.1
300707	2.1
300804	2.1
301206	2.1
301212	2.1
301412	2.1

Table 11: PIDs and their new thickness from the best design of the first optimisation stage for the side door

As for configuration 3, the patches that are far away from all thickened patches

from the first optimisation are removed for the second stage. Unlike for configuration 3 however, the side door is given the possibility to obtain new patches outside the initially identified sensitive areas. This decision is based on the fact that the modal behaviour of the model can change when adding thickness and that the initial sensitivity analysis might not be accurate for the thickened model.

The method for updating the side door for the second optimisation leads to 85 available patches to be thickened, 11 of which having already been thickened once. The model used for the second optimisation stage of the side door is shown in Fig. 43

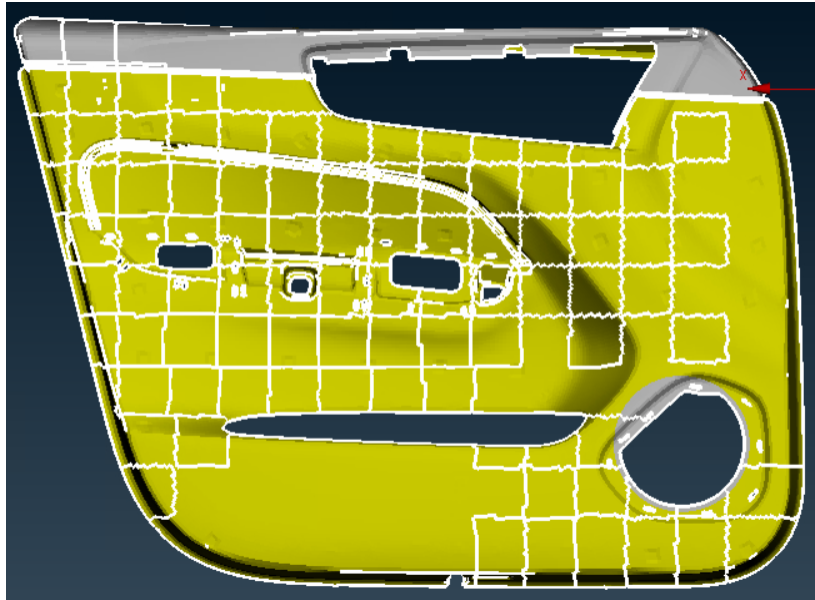


Figure 43: Available patches for the second optimisation stage for the side door

5 Results

This chapter presents the scatter plots from each optimisation stage where the optimal design is denoted as *Opt*. The thickened areas of the optimal design at the final optimisation stage are also presented as well as the final thicknesses of the patches.

5.1 Configuration 3

The objective functions of geometric variation and dynamic response are plotted against each other in a scatter plot. The scatter plots for the four stages of the optimisation of configuration 3 are shown in Figs. 44, 45, 46 and 47. The optimal design (*Opt*) is manually chosen from the pareto front in modeFRONTIER.

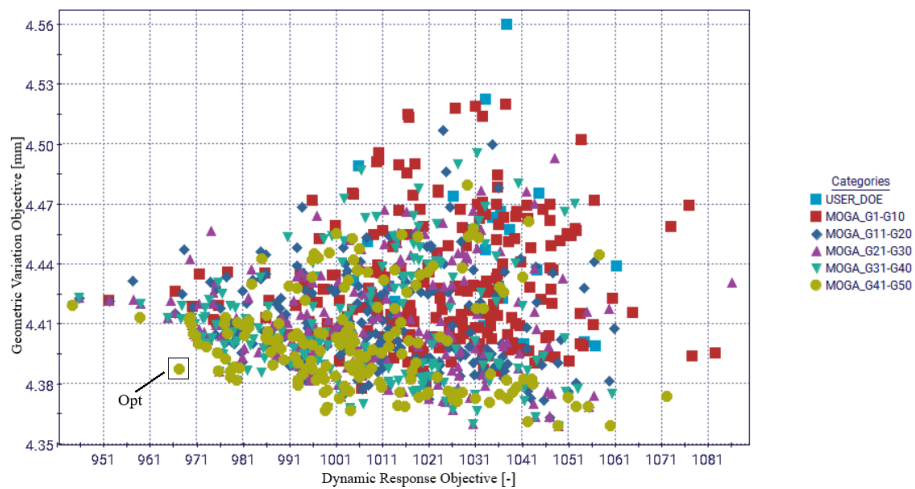


Figure 44: Scatter plot from the first optimisation stage for configuration 3

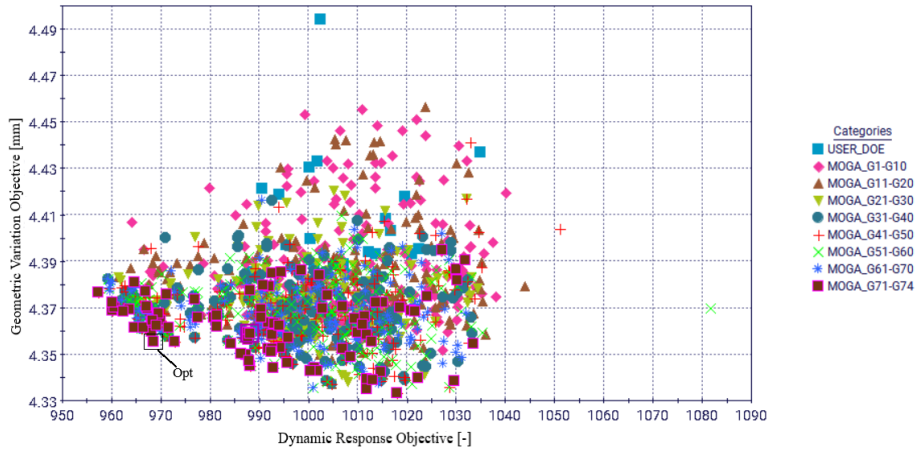


Figure 45: Scatter plot from the second optimisation stage for configuration 3

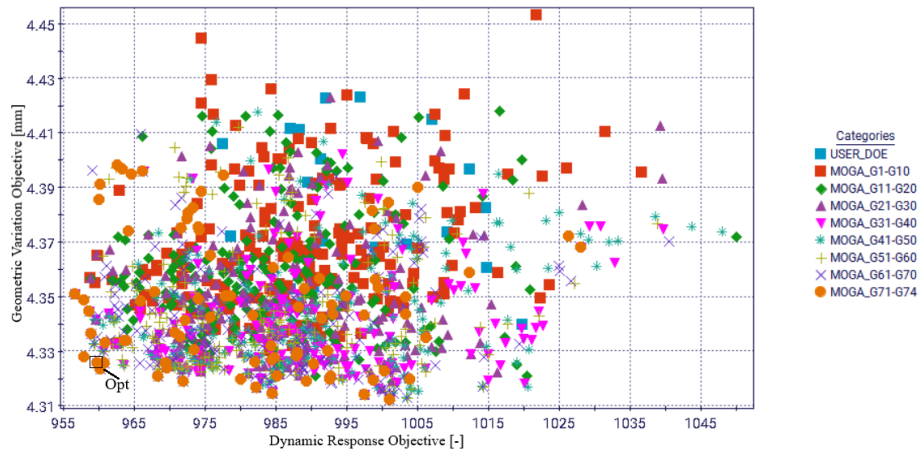


Figure 46: Scatter plot from the third optimisation stage for configuration 3

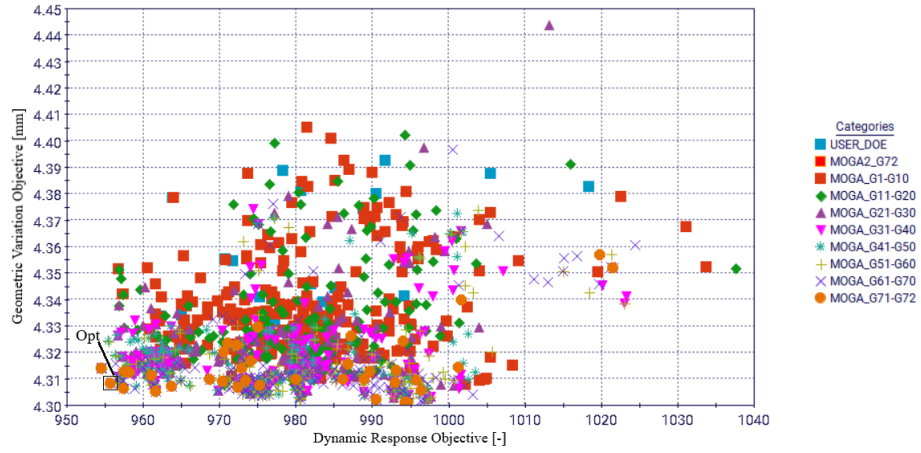


Figure 47: Scatter plot from the fourth optimisation stage for configuration 3

The final version of configuration 3 is shown in Fig. 48. The new patches are marked with red and their PIDs can be found in Table 48. A complete list of the thickened PIDs, their final thickness and in which stages they were thickened is presented in Table 48. 24 patches are thickened in total, four of which are thickened twice.

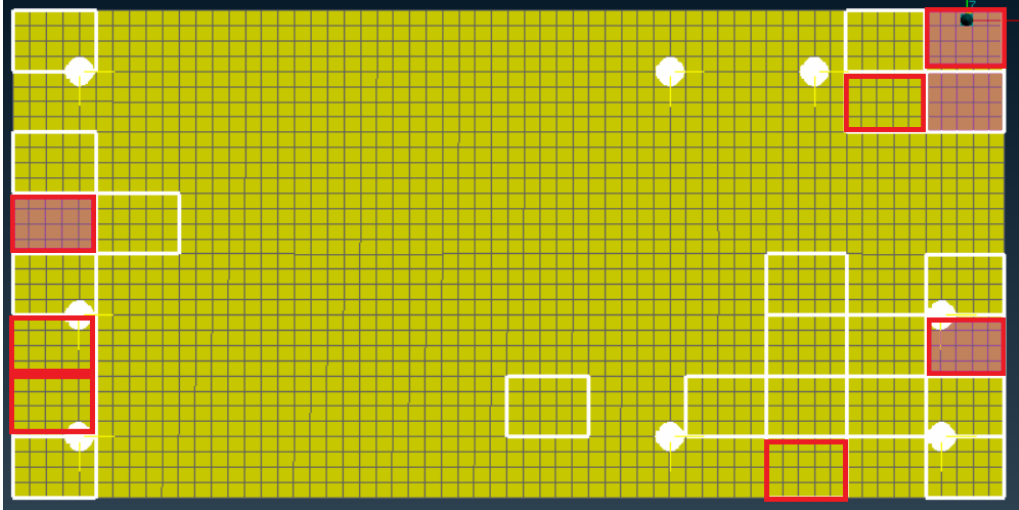


Figure 48: Thickened areas after the final optimisation stage for configuration 3. Patches added in the last stage have red edges and the purple patches are 4 mm thick.

PID	100104	100106	100107	101008	101102	101201	101206
Thickness (mm)	4	3.5	3.5	3.5	3.5	4	4

Table 12: PIDs and their new thickness from the best design of the final optimisation stage

PID	Thickness (mm)	Selected in stage
100101	3.5	1
100103	3.5	2
100104	4	1 & 4
100105	3.5	3
100106	3.5	4
100107	3.5	4
100108	3.5	1
100204	3.5	2
100707	3.5	3
100907	3.5	2
101005	3.5	1
101006	3.5	3
101007	3.5	1
101008	3.5	4
101101	3.5	3
101102	3.5	4
101106	3.5	3
101107	3.5	2
101201	4	1 & 4
101202	4	1 & 2
101205	3.5	2
101206	4	3 & 4
101207	3.5	2
101208	3.5	3

Table 13: The PIDs and thicknesses from the optimisation of configuration 3

5.2 Side door

The scatter plots for the two optimisation stages in Figs. 49 and 50, respectively, show the objective values for geometric variation and dynamic response. In Figs. 49 and 50, the optimal design is marked as *Opt*. However, further designs on the Pareto front are also marked to illustrate other possible candidates that are considered to be optimal as well. The optimal patches to these designs, as well

as *Opt*, are shown in Fig. 51 and 52 for the different optimisation stages.

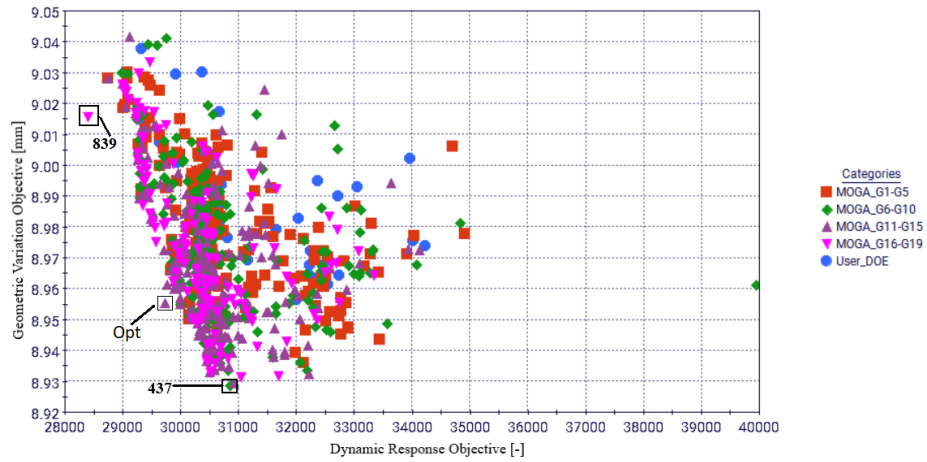


Figure 49: Scatter plot from the first optimisation stage for the side door

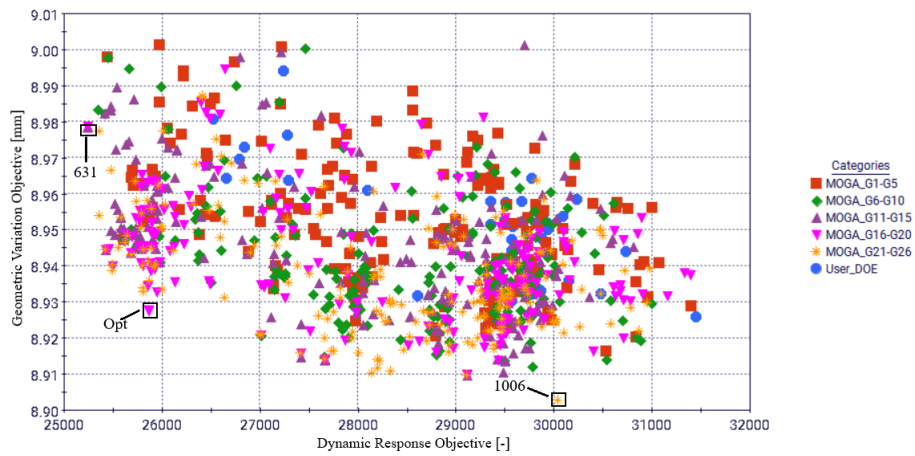
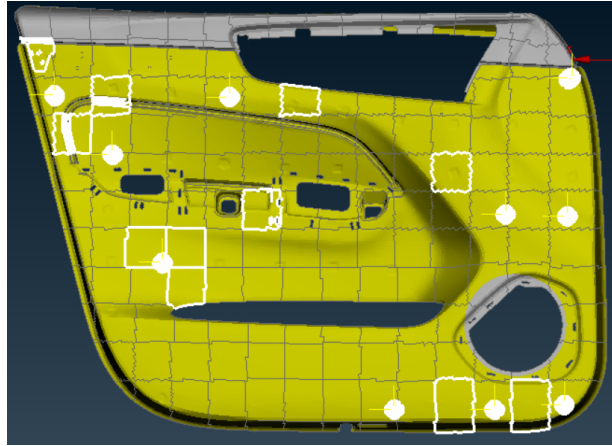
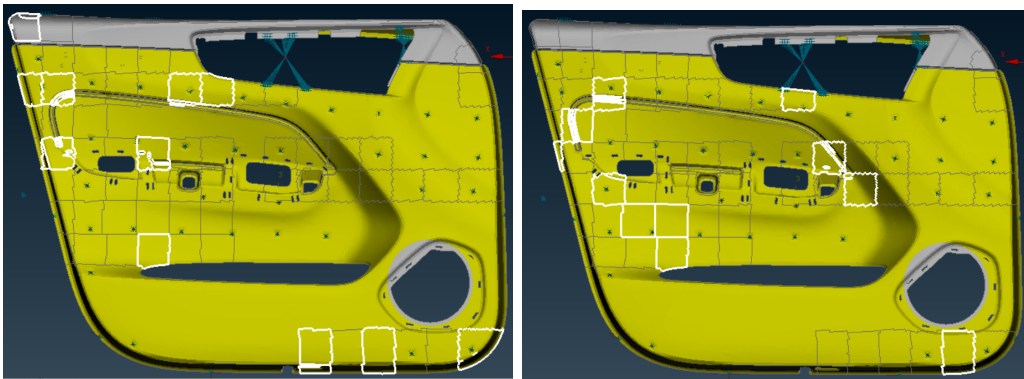


Figure 50: Scatter plot from the second optimisation stage for the side door



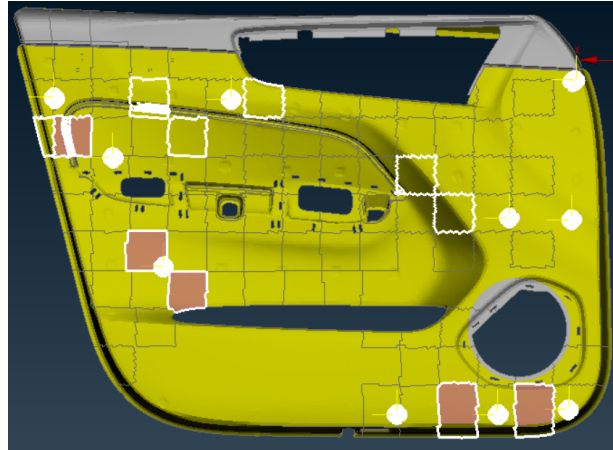
(a) Opt



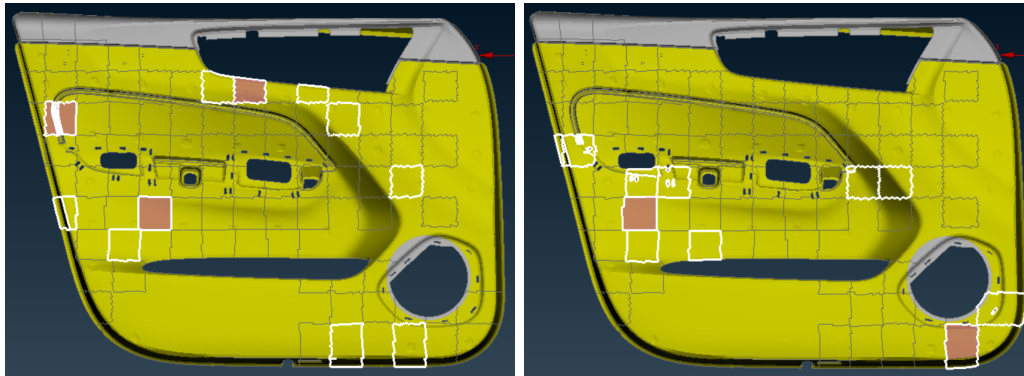
(b) 839

(c) 437

Figure 51: Designs on the Pareto front from the first optimisation stage for the side door



(a) Opt



(b) 631

(c) 1006

Figure 52: Designs on the Pareto front from the second optimisation stage for the side door

The resulting model from the final optimisation of the side door can be seen in Fig. 53. Five patches were selected in both stages and are therefore 2.4 mm thick. All selected PIDs, their final thickness and in which stage they were thickened is presented in Table 14.

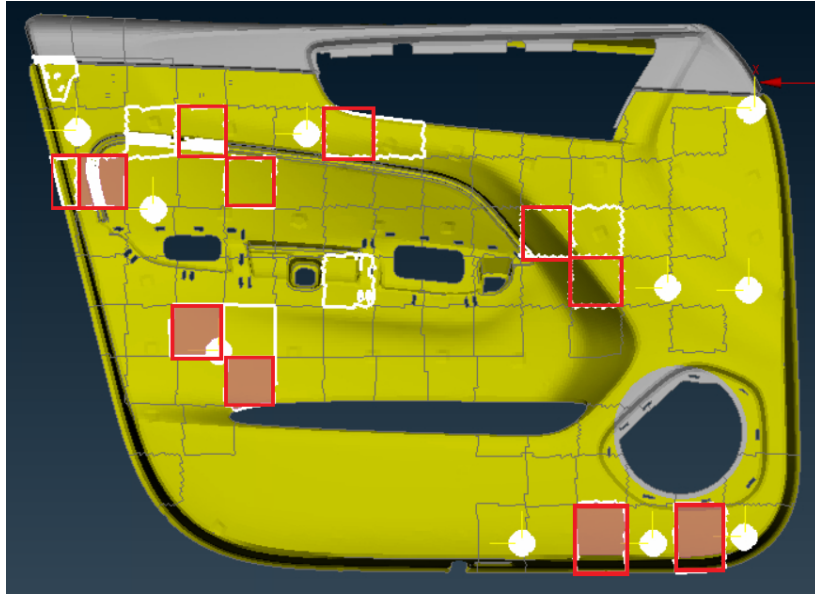


Figure 53: Thickened areas after the final optimisation stage for the side door. Patches added in the last stage have red edges and the purple patches are 2.4 mm thick.

PID	Thickness (mm)	Selected in stage
300102	2.1	1
300105	2.1	2
300205	2.4	1 & 2
300304	2.1	1
300404	2.1	2
300408	2.4	1 & 2
300505	2.1	2
300508	2.1	1
300509	2.4	1 & 2
300704	2.1	2
300707	2.1	1
300804	2.1	1
301106	2.1	2
301206	2.1	1
301207	2.1	2
301212	2.4	1 & 2
301412	2.4	1 & 2

Table 14: The PIDs and their thicknesses from the optimisation of the side door

6 Discussion

6.1 Configuration 3

The scatter plots in Figs. 44, 45, 46 and 47, show that the objective values for each design, including the optimal design, are reduced for each generation and each optimisation stage. This is reasonable since adding thickness increases the stiffness. The cluster of designs from the generations also seem to become less spread out for every optimisation stage. These observations indicate that the optimisation method of adding thickness in multiple stages improves the performance by minimising the dynamic response and geometric variation.

If another design on the Pareto front would have been chosen to be the optimal design to continue with in the next optimisation stages, the results of the thickened patches would have been different. This would not necessarily indicate that one design is better than the other, but rather if the dynamic response is more important to minimise than the geometric variation or vice versa. Additionally, one can assume, based on previous projects at VCC, that some patches in the optimal design appear in other Pareto designs.

The theory that it would be optimal to thicken the model around the fasteners cannot be considered as verified or disproved based on the final results for configuration 3. The model is thickened around some fasteners whereas the areas around other fasteners have remained with the nominal thickness after the optimisation. This can be an indication that the global stiffness of the model is more important than the local stiffness when minimising for squeak and rattle.

Since adding thickness to the model improves the stiffness at the same time as it changes the general behaviour of the model, it is not certain that the initial sensitivity analysis is valid for the model with thickened areas. Due to this, it could be argued that more areas than the ones identified in the sensitivity analysis should have been added in the optimisation stages.

When comparing the thickened areas in the final model in Fig. 48 and the one

from the sensitivity analysis in Fig. 29, there are some patterns that are similar and some that are not. Patch number 4, see Fig. 19, from the sensitivity analysis is not thickened in the final model. The sensitive area around patch 26 at the bottom of the model did not get many thickened patches in the optimisation either. One explanation for this is that according to Fig. 18, these areas were the least sensitive of the areas identified in the sensitivity analysis. The more sensitive areas such as the areas at the upper right corner and along the left vertical side were thickened in the optimisation similarly to the initial analysis. However, one should not forget that the result from the sensitivity analysis is not fully comparable to the optimised results since the behaviour of the model changes when adding thickness.

The most noticeable behaviour of the model in both the sensitivity analysis and the topometry optimisation is that the model should be thickened around the edges rather than the middle in order to decrease the risk of squeak and rattle.

6.2 Side door

Similar to configuration 3, the observations made from the scatter plots in Figs. 49 and 50 show that the developed method of applying topometry optimisation in multiple stages, minimises the dynamic response and geometric variation. A relation between fastener location and thickened areas cannot be found in Fig. 51a, which is why the fasteners are not taken into account in the second optimisation stage. It can therefore be stated that the stiffness for global behaviour seems to be more important than the local stiffness close to the fasteners.

Compared to configuration 3, the edges and corners in the optimal design from the final optimisation stage for the side door, seen in Fig. 53, are not targeted to become thicker and more stiff. It rather seems like increasing the stiffness is more necessary where the model is more complex, such as nearby holes or where indentation and other details are present. The differences may indicate that the side door cannot be directly compared to configuration 3 in terms of topometry optimisation, perhaps due to the complexity of the side door model.

Two further Pareto designs are marked in the scatter plots in Figs. 49 and 50. The corresponding patches are depicted in Figs. 51bc and 52bc, respectively.

These designs illustrate the optimal designs if one were to prioritise either the dynamic response objective (839 and 631) or the geometric variation objective (437 and 1006). Several thickened patches in these extreme designs are visible in the optimal design *Opt*. *Opt* from the first optimisation stage, seen in Fig. 52a, seems to, more or less, be a combination of design 839 and 437. However, the combination of design 631 and 1006 are harder to distinguish in *Opt* from the second optimisation stage in Fig. 52a.

Comparing the thickened areas after the final optimisation stage with the identified areas in the initial sensitivity analysis show some similarities and some significant differences. The most obvious difference can be seen in the bottom right corner of the side door, where two patches far from any sensitive area, have been thickened twice. These patches would not have been candidates for the optimisations if fasteners were not present in the surrounding area. The lack of tendency for thickness around the fasteners in other areas could suggest that there are areas that were excluded after the sensitivity analysis, which would have been thickened in an optimal solution. It is possible that the patches in the bottom right corner were not identified due to limitations with using a Plackett-Burman design for the sensitivity analysis.

Several patches have most likely been neglected in the sensitivity analysis due to using a Plackett-Burman design with foldover. Only nonlinearities imposed by the two-factor interactions are taken into account. Usually, a two-level design is not sufficient to detect all nonlinearities. The lack of detecting nonlinearities may be a reason to why some patches are neglected in the early stage, although an acceptable approximation in engineering is to assume that the system response is linear in an isolated single parameter change, though in reality it is not.

Due to time limitation, only two optimisation stages were performed. According to Table 6, two stages correspond to an increase in mass with approximately 2%. However a limit of 5% increase in mass is set in Eq. 11. Performing further optimisation stages would result in a higher mass increase according to Eq. 11. With a 5% limit in mind, this would also result in lower objective values.

7 Conclusions

The results from the multidisciplinary topometry optimisation indicate that the side door cannot be fully represented by configuration 3. The areas that need to be stiffened varies as the results for configuration 3 show that areas close to the edges and corners need more stiffness while the areas of the side door that need more stiffness are located where complexity of the model is present. One should therefore use more realistic simplified geometries that better represent the corresponding full models.

Further relevant findings from this thesis work are the verification of reduced geometric variation and dynamic response by applying topometry optimisation in multiple stages. Thus, is the developed methodology successful in terms of reducing the risk for squeak and rattle. However, the underlying factors for the results in the sensitivity analysis, such as the choice of experimental design, are not fully accurate which result in neglecting some areas that need to be stiffened in the optimisation. Additionally, increasing the stiffness globally has a larger effect on the objective values than increasing the stiffness locally close to the fasteners.

8 Sources of error

Possible sources of error include results from the sensitivity analysis, the position of fasteners in the ANSA and RD&T model, the activated planar fasteners and the number of studied geometries in this thesis work. These sources of error may therefore have an influence on the results and the conclusions made in this thesis.

The sensitivity analysis is performed with only two-factor interactions and further interactions are therefore neglected. These interactions are most probably present and affects the results.

Since the system is very sensitive to changes of multiple design variables in the sensitivity analysis, it cannot be stated that a Plackett-Burmann design with foldover would give perfectly consistent results as this was one of the initial encountered problems. However, to get more consistent results, the number of interactions have been reduced instead.

As previously discussed, the behaviour of the model, e.g. the modal behaviour, changes when varying the thickness of some patches. The sensitivity analysis performed prior to the optimisation might not be fully applicable in the latter optimisation stages. In configuration 3, the area allowed to vary in thickness in the latter optimisation stages should, in fact, be extended as this might lead to thicker areas connecting the sensitive areas found from the sensitivity analysis. This was, however, considered for the side door model.

The geometries were provided in this thesis work and both the RD&T and ANSA model should be equivalent. However, for configuration 3, the positions of the fasteners were not aligned in the RD&T and ANSA models. Furthermore, it was critical to reduce the number of planar fasteners in configuration 3 and the side door model. The choice of the number of activated planar fasteners, the position of these and the direction may have affected both the geometric variation and dynamic response.

Due to complications with the provided models and limited time, only one simplified geometry and one full model were studied. It is therefore not fully correct to draw general conclusions based on these two models.

9 Future recommendations

Further simplified geometries and full models, available at VCC, can be explored. Comparing those results to the ones from this thesis work would add further credibility to the developed method. Applying the method to additional geometries could bring more insight on the behaviour around the fasteners, how well the results from the sensitivity analysis coincides with the thickened areas in the final model as well as similarities between different geometries to draw general conclusions.

An additional recommendation is to convert the simplified solutions made in this thesis work to a manufacturing case. Validation with physical measurements can be made to study if the squeak and rattle risk for the optimised designs is lower than for the baseline designs.

Since pre-processing was time consuming, an automated method of creating the grid pattern on a model in ANSA can be developed to make the further work more time efficient. Furthermore, to avoid creating a new model in ANSA for the different optimisation stages, it is possible to develop a method were all patches are allowed to be possible candidates but only a few neighborhoods are acceptable.

The algorithm used for the DOE in the sensitivity analysis can be further explored to account for more interactions as these are presumably important. Definite screening designs can be studied to consider nonlinear effects. Further optimisation algorithms can also be explored, such as gradient based algorithms.

Additional constraints can be elaborated, one of them being a directional constraint which allows the thickened patches to grow in a certain direction. This might lead to a more user defined pattern which might be useful if, for example, manufacturing constraints are taking into account.

Another suggestion for future work would be to study the design of ribs or other alternatives to replace the optimal thickened areas based on this method. Such work should include consideration of the limitations caused by the manufacturing and assembly methods that are used.

References

- [1] Allemang, R. (2003), *The Modal Assurance Criterion - Twenty Years of Use and Abuse*. Cincinnati, Ohio: University of Cincinnati.
- [2] Batchu, S. (2015) *Spring Elements In Nastran* Retrieved October 19, 2020, from <https://www.stressebook.com/spring-elements-in-nastran/>
- [3] Bayani, M., Wickman, C., Lindkvist, L. & Söderberg, R. (2020), *Squeak and rattle prevention by geometric variation management using a two-stage evolutionary optimisation approach. International Mechanical Engineering Congress and Exposition*. Portland, Oregon, USA: Advanced Materials Science and Engineering (ASME).
- [4] Benhayoun, I., Bonin, F., Milliet de Faverges, A., & Masson, J. (2017) *Simulation & Optimization Driven Design Process for S&R Problematic - PSA Peugeot Citroën Application for Interior Assembly. SAE International - Noise and Vibration Conference and Exhibition*. <https://doi.org/10.4271/2017-01-1861>
- [5] Carnell, R. (2020) *Basic Latin hypercube samples and designs with package lhs*. Retrieved January 18, 2021, from https://cran.r-project.org/web/packages/lhs/vignettes/lhs_basics.html#X
- [6] Chen, H. et al., (2020). *Structural Modal Analysis and Optimization of SUV Door Based on Response Surface Method*. Wuhan, China, Hubei Key Laboratory of Advanced Technology for Automotive Components, Wuhan University of Technology. <https://doi.org/10.1155/2020/9362434>
- [7] *Damped Harmonic Oscillator Scenario*. (2017). Retrieved January 11, 2021, from: <https://physics.stackexchange.com/questions/340740/damped-harmonic-oscillator-scenario>
- [8] *Dynamic Stiffness, Compliance, Mobility and more....* (August 29, 2019) retrieved September 17, 2020, from: <https://community.sw.siemens.com/s/>

article/dynamic-stiffness-compliance-mobility-and-more

- [9] ESTECO SpA (2019) *modeFRONTIER User Guide, Create, configure and run a DOE*, Trieste, Italy: AREA Science Park, ESTECO SpA
- [10] ESTECO SpA (2019) *modeFRONTIER User Guide, Incremental Space Filler*, Trieste, Italy: AREA Science Park, ESTECO SpA
- [11] ESTECO SpA (2019) *modeFRONTIER User Guide, Plackett-Burman*, Trieste, Italy: AREA Science Park, ESTECO SpA
- [12] Fuwen, H. (2014), *Location Issues of Thin Shell Parts in the Reconfigurable Fixture for Trimming Operation* (Vol. 6) Beijing, China: North China University of Technology. ISSN 2175-9146 <https://doi.org/10.5028/jatm.v6i3.321>
- [13] He, J. & Fang, Z-F. (2001), *Modal Analysis*. Oxford, United Kingdom: Butterworth-Heinemann. <https://doi.org/10.1016/B978-0-7506-5079-3.X5000-1>
- [14] Katrnak, T., Juracka J. (2016), *Topometry FEM optimization of the wing structure of the transport aircraft*. Brno, Czech republic. Taylor & Francis Group. <https://doi.org/10.3846/16487788.2016.1266819>
- [15] Kavarana, F. & Rediers, B. (2001), *Squeak and Rattle - State of the Art and Beyond*. Troy, Michigan, USA: Defiance Testing & Engineering. <https://doi.org/10.4271/1999-01-1728>
- [16] Krishnaswamy, A. & Sathappan, C. (2020). *Multidisciplinary Optimisation of Geometric Variation and Dynamic Behaviour for Squeak & Rattle*. (Master Thesis, Divison of Product Development, Department of Industrial and Materials Science, Chalmers University of Technology, Gothenburg, Sweden)
- [17] Kulkarni, S. & Ratnam, D. (2019). *Multidisciplinary Optimization of Geometric Variation Analysis & Modal Behaviour for Squeak & Rattle Prevention*. (Master Thesis, Divison of Product Development, Department of Industrial and Materials Science, Chalmers University of Technology, Gothenburg, Sweden)

- [18] Kwon, Y. Kwon, S. Kim, S. Lee, J. (2015) *Position and Thickness Optimization of Ribs for Ventilation Covering Using the Micro Genetic Algorithm with an Interpolated Smooth Objective Function*. Daegu, Republic of Korea. Hindawi Publishing Corporation. <https://doi.org/10.1155/2015/859653>
- [19] Lam, Y.C. S. Santhikumar, S. (2003) *Automated Rib Location and Optimization for Plate Structures*. Singapore. <https://doi.org/10.1007/s00158-002-0270-7>
- [20] Li, W. Zheng, A., You, L., Yang, X., Zhang, J. & Liu, L. (2017) *Rib-reinforced Shell Structure* (Vol.36). China, UK. John Wiley & Sons Ltd. <https://doi.org/10.1111/cgf.13268>
- [21] Lindkvist L. (2017). *Lecture in PPU080 Advanced Computer Aided Design: Geometry Assurance 1 - Robust Design & Variation Simulation*. Chalmers University of Technology, Gothenburg, Sweden
- [22] Montgomery, D.C.(2012) *Design and Analysis of Experiments (8th edition)*. John Wiley & Sons, Inc.
- [23] Mourelatos, Z.P. & Liang, J. (2005). *A Reliability-Based Robust Design Methodology*. SAE Transactions, 114, 848-858. Retrieved January 22, 2021, from <http://www.jstor.org/stable/44725119>
- [24] Mozumder, C. (2010) *Topometry Optimization of Sheet Metal Structures for Crashworthiness Design Using Hybrid Cellular Automata*. (Dissertation, Aerospace and Mechanical Engineering, Graduate School of the University of Notre Dame)
- [25] Narayana, N. (2011) *A Finite Element Method for Effective Reduction of Speaker-Borne Squeak and Rattle Noise in Automotive Doors*. SAE Technical Paper 2011-01-1583. <https://doi.org/10.4271/2011-01-1583>
- [26] Ottosen, N. & Peter, G.(1992) *Introduction to the Finite Element Method*. London, United Kingdom: Pearson Education.
- [27] *Optimization-driven design*. Retrieved: September 17, 2020, from: <https://www.esteco.com/technology/optimization-driven-design>

- [28] Pedersen, B. (2018), *Conceptual Dynamic Analysis of a Vehicle Body*. (Master Thesis, Division of Structural Mechanics, Department of Construction Sciences LTH, Lund University, Lund, Sweden).
- [29] Poles, S., Rigoni, E. & Robic, T. (2004), *MOGA-II performance on noisy optimization problems*, Ljubljana, Slovenia: Department of Intelligent Systems, Jozef Stefan Institute.
- [30] *PSHELL*. Retrieved: October 19, 2020, from: <https://knowledge.autodesk.com/support/nastran/learn-explore/caas/CloudHelp/cloudhelp/2019/ENU/NSTRN-Reference/files/GUID-075E0B52-7716-4BCB-9A3D-CE81C9290123-htm.html>
- [31] RD&T *Main steps RD&T*. (n.d.). Retrieved September 17, 2020 from: <http://www.rdnt.se/steps.html>
- [32] RD&T *The tool RD&T*. (n.d.). Retrieved September 17, 2020 from: <http://www.rdnt.se/tool.html>
- [33] Schmidt, R., Voigt, M. & Mailach, R. (2019) *Latin Hypercube Sampling-Based Monte Carlo Simulation: Extension of the Sample Size and Correlation*. Cham, Switzerland. Springer. https://doi.org/10.1007/978-3-319-77767-2_17
- [34] Siemens *Natural Frequency and Resonance*. (November 2, 2019). Retrieved: September 17, 2020, from: <https://community.sw.siemens.com/s/article/Natural-Frequency-and-Resonance>
- [35] Son, G-H., Cho, S-J. & Park, Y-J. (2019), *Rib Design for Improving the Local Stiffness of Gearbox Housing for Agricultural Electric Vehicles*. Seoul, Korea, Department of Biosystems and Biomaterials Science and Engineering, College of Agriculture and Life Sciences, Seoul National University. <https://doi.org/10.3390/app9214571>
- [36] Sundararajan, K. *Design of Experiments - A Primer* (n.d.). Retrieved: September 17, 2020, from: <https://www.isixsigma.com/tools-templates/design-of-experiments-doe/>

- [37] Tavcar, J. & Duhovnik, J. (2014), *Case study analysis and genetic algorithm adaptation for job process planning and scheduling in batch production*. Journal of design research, vol. 12, no 1/2, pp 52-77. Ljubljana, Slovenia: Faculty of Mechanical Engineering, University of Ljubljana
- [38] Zhen, H. & Zhihong, Z. *An application study on six sigma tolerance design*. Department of Industrial Engineering, School of Management Tianjin University ,Tianjin, China. Retrieved September 17, 2020 from <http://www.paper.edu.cn/scholar/showpdf/NUz2gN1INTj0IxeQh>

Appendix A Work distribution and time plan

A.1 Work distribution

Activity	Minh Tang	Karl Lindkvist
Setting up the report template	50%	50%
Literature review	50%	50%
Written sections	Acknowledgements, 1.2, 1.3, 1.4, 2.1, 2.2.1, 2.2.2, 2.2.3, 2.2.5, 2.5.1, 2.5.3, 2.7.1, 3.1i, 3.1.1, 3.1.2, 3.1.3, 3.1.4 (50%), 3.2i (70%), 3.2.1, 3.2.2, 3.3.4, 3.5.2, 3.5.3, 3.6, 4i, 4.1, 4.6i (50%), 4.6.2, 5i, 5.1 (50%), 6.1 (30%), 8, 9 (60%), 6.2 (70%), 7 (50%), References (50%)	Abstract, Sammanfattning, 1.1, 2.2i, 2.2.4, 2.3, 2.3.1, 2.3.2, 2.4, 2.5i, 2.5.2, 2.5.4, 2.6i, 2.6.1, 2.7.2, 3i, 3.1.4 (50%), 3.2i (30%), 3.3, 3.3.1, 3.3.2, 3.3.3, 3.3.5, 3.4, 3.5i, 3.5.1, 4.2, 4.3, 4.4, 4.5i, 4.5.1, 4.5.2, 4.5.3, 4.5.4, 4.5.5, 4.6i (50%), 4.6.1, 5.1 (50%), 6.1 (70%), 9 (40%), 6.2 (30%), 7 (50%), References (50%)
Creating a Gantt chart	-	100%
Creating a table for work distribution	100%	-

Table 15: Work distribution of the thesis report. i denotes the introductory part of the section

Activity	Minh Tang	Karl Lindkvist
Development of the methodology	50%	50%
Development of the initial workflows in software	50%	50%
Modelling	60%	40%
Simulation to find weightings	100%	-
Perform sensitivity analysis	100%	-
Perform topometry optimisation	-	100%

Table 16: Work distribution of the practical work

A.2 Project plan and outcome

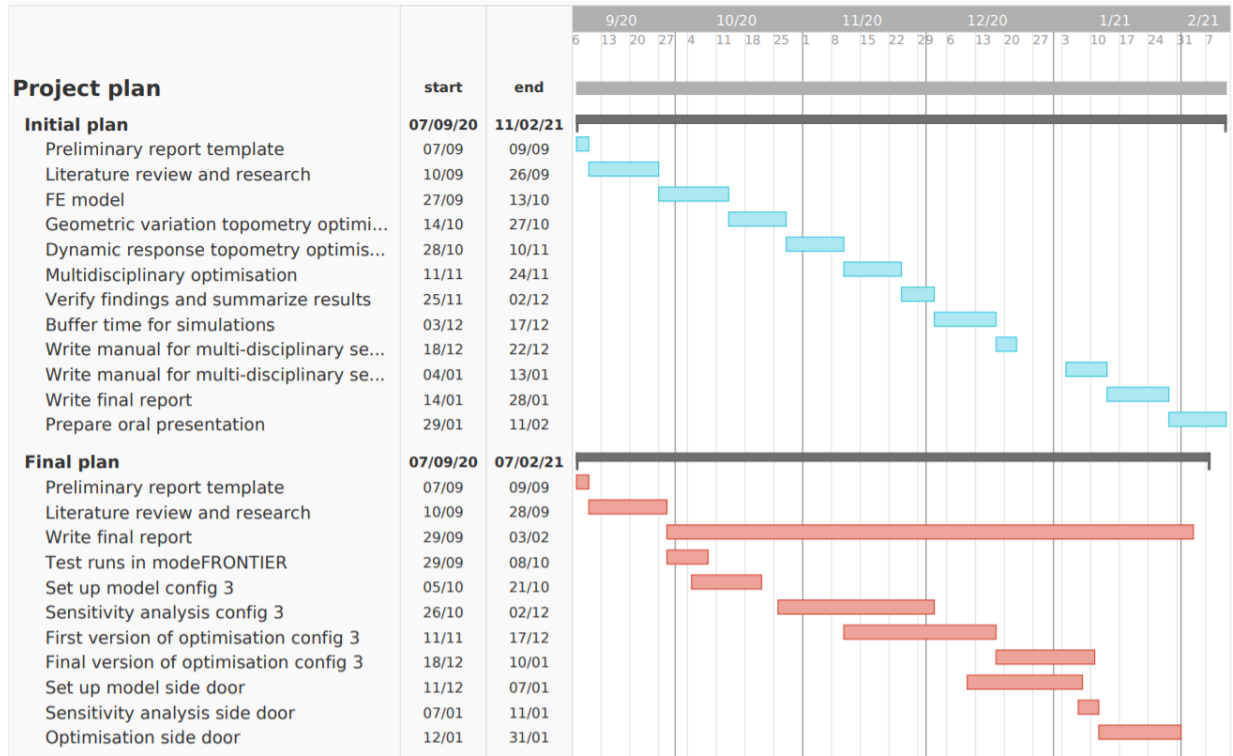


Figure 54: Project plan